Development of biodegradable nanobeads as a novel drug delivery system for the treatment of tuberculosis using the zebrafish model.

Terje Ricardo Selnes Kolstad

Thesis for the Master's degree in Molecular Biosciences

Department of Molecular Biosciences
Faculty of Mathematics and Natural Sciences

UNIVERSITY OF OSLO

June 2013

Acknowledgements

First and foremost I would like to thank Prof. Gareth Griffiths for introducing me to the world of science and for sharing with me, some of the encyclopedic wealth of knowledge that he posesses.

I would also thank all the members of my group; Jørgen, Lilia, Jon, Bård, David, Lasse, Raja, Martin, Carina, Eva and in particular my friend and supervisor Federico Fenaroli. I am also indebted to Gerbrand Koster of Oddmund Bakke's group for his willigness to teach me fluorescence microscopy and image processing.

A special mention goes to four of my fellow students through five great years; thank you Olav, Ivan, Lars and Kristian.

Without the total support of my family I would not be where I am today and therefore, I dedicate this thesis to them.

Oslo, June 2013

Terje Ricardo Selnes Kolstad

Abstract

Tuberculosis (TB) is a disease caused by the bacterium *Mycobacterium tuberculosis,* a pathogen that has accompanied mankind throughout its far and recent history. Current TB-therapy consists of two treatment phases, one initial phase where a cocktail of four frontline anti-tubercular drugs are administered daily for a minimum of two months followed by a continuation phase where two or more drugs are taken for a minimum of four months. The extensiveness of the treatment is a problem as it becomes very costly and hampers patient lifestyle. In turn, this may lead to patient non-compliance and an increased probability of the emergence of drug resistant strains. There is thus a great need for developing new drugs and to improve the efficiency of current drugs. Our group has developed a method for encapsulating one of the frontline anti-TB drugs, rifampicin (RIF), in the biodegradable polymer Poly-Lactic-co-Glycolic-Acid (PLGA). The idea behind encapsulating the drug is to promote its gradual release, increase its residence time in the body, to promote a natural co-localization between drug and pathogen and by doing so, enhance the therapeutic effect of the drug. The main goal of my master project has been to develop and apply methods for measuring the effect of these PLGA-RIF-nanoparticles on zebrafish challenged with mycobacterial infection. The experiments reveal a decrease in bacterial burden accompanied by a significant increase in the survival of zebrafish larvae treated with these nanoparticles compared to their free-drug counterparts. This thesis therefore substantiates the claim that nanoparticle-based therapy holds real promise for the successful treatment of TB.

Contents

Abbreviations

ADC	Albumin Dextrose Catalase
AIDS	Acquired Immunodeficiency Syndrome
BCG	Bacillus Calmette-Guèrin
CD	Cluster of Differentiation
CFU	Colony Forming Units
DC	Dendritic Cell
DCM	Dichloromethane
DMSO	Dimethyl Sulfoxide
DPF	Days Post-Fertilization
DPI	Days Post-Infection
DPT	Days Post-Treatment
EDTA	Ethylenediaminetetraacetic acid
EMBL	European Molecular Biology Laboratory
EPR	Enhanced permeation and retention effect
FPC	Fluorescent Pixel Count
HIV	Human Immunodeficiency Virus
IFNγ	Interferon Gamma
IL-1β	Interleukin-1 Beta
INH	Isoniazid
Int.Den	Integrated Density
M.marinum	*Mycobacterium marinum*
M.tuberculosis	*Mycobacterium tuberculosis*
MDR-TB	Multi-drug-resistant tuberculosis
MHC II	Major histocompatibility complex II

NP	Nanoparticle
O/W	Oil-in-Water emulsion
OD_{600}	Optical Density at 600 nm
PBS	Phosphate Buffered Saline
PEG	Polyethylene glycol
PLGA	Poly-Lactide-Co-Glycolide
PVA	Polyvinyl Alcohol
PVP	Polyvinylpyrrilidone
PZA	Pyrazinamide
Rag	Recombination activating genes
RIF	Rifampicin
SDS	Special Diet Services
SEM	Scanning Electron Microscope
SPA receptors	Surfactant protein A-receptors
TB	Tuberculosis
TEM	Transmission Electron Microscope
TLR	Toll-like receptor
TNFα	Tumor necrosis factor alpha
WHO	World Health Organization

1 Introduction

1.1 A brief history of tuberculosis

Phthisis or consumption, the process in which the substance of a thing is completely destroyed, was identified by Hippocrates (460-377 BC) as the most widespread, most lethal disease of its time [1]. Findings of tubercular decay in Egyptian mummies dating back to 3000 BC [2] add further evidence that tuberculosis (TB) has accompanied mankind for a very long time. During the 18th and 19th century the disease ravaged Europe and North-America earning the nickname "Captain among these men of death," and it was during this time that one began to understand the pathophysiology of the disease [3]. In 1882 Robert Koch identified *Mycobacterium tuberculosis* as the causative agent of TB [4] and about 40 years later Albert Calmette and Camille Guérin had developed a vaccine (BCG) by serial passage of the closely related species *Mycobacterium bovis* [5]. From 1952-1961, four new frontline anti TB-drugs were introduced, that when used in combination, has a treatment success rate of up to 87% [6]. At present, 11 new vaccines and several new or re-purposed TB-drugs are advancing in clinical trials and regulatory review. But despite this continual effort to develop tools with which to fight the disease, the World Health Organization (WHO) could in 2012 report 1.4 million deaths and 8.7 million new cases of TB [6]. Furthermore, it is estimated that about one third of the world's population is latently infected with TB [7].

1.2 Initial infection

Tuberculosis is an airborne disease. A susceptible host may contract the disease by inhaling tiny water droplets containing the bacilli that are released when an infected host coughs or sneezes [8]. The bacilli need to reach the site of gas exchange, the alveoli, and avoid being trapped in the mucosal layers of the upper respiratory tract. Once in the alveoli the bacilli will be taken up by professional phagocytes, in particular alveolar macrophages [9] (FIG.1). There are many different receptors involved in the uptake of the bacilli, including TLRs, CD14, complement receptors, mannose receptor, SPA receptors, scavenger receptors and after the onset of adaptive immunity, Fc-receptors [10-16]. It is believed that once having phagocytosed the bacilli, the macrophages infiltrate the subtending epithelial layer causing a local inflammation [17]. This inflammation will attract mononuclear cells from surrounding

blood vessels, thus providing new host cells for the expanding bacterial population and establishing a primary lesion [18].These early lesions form the structural basis for what eventually will develop into a tubercle, or granuloma – the hallmark structure of TB [19]. Alternatively, the bacilli can be taken up by dendritic cells (DCs) and transported to the nearest lymph node for activation of the adaptive immune system [20]. It is believed that through the lympho-hematogenous route the bacilli may establish secondary TB-lesions throughout the body [21]. This disease state is termed miliary tuberculosis and is particularly lethal. The mortality rate of miliary tuberculosis, which most often affects young children and HIV/AIDS patients [22], is 30% even when treated [23]. About 80-85% of all cases are pulmonary TB wherein the bacilli remain exclusively in the respiratory tissue [24].

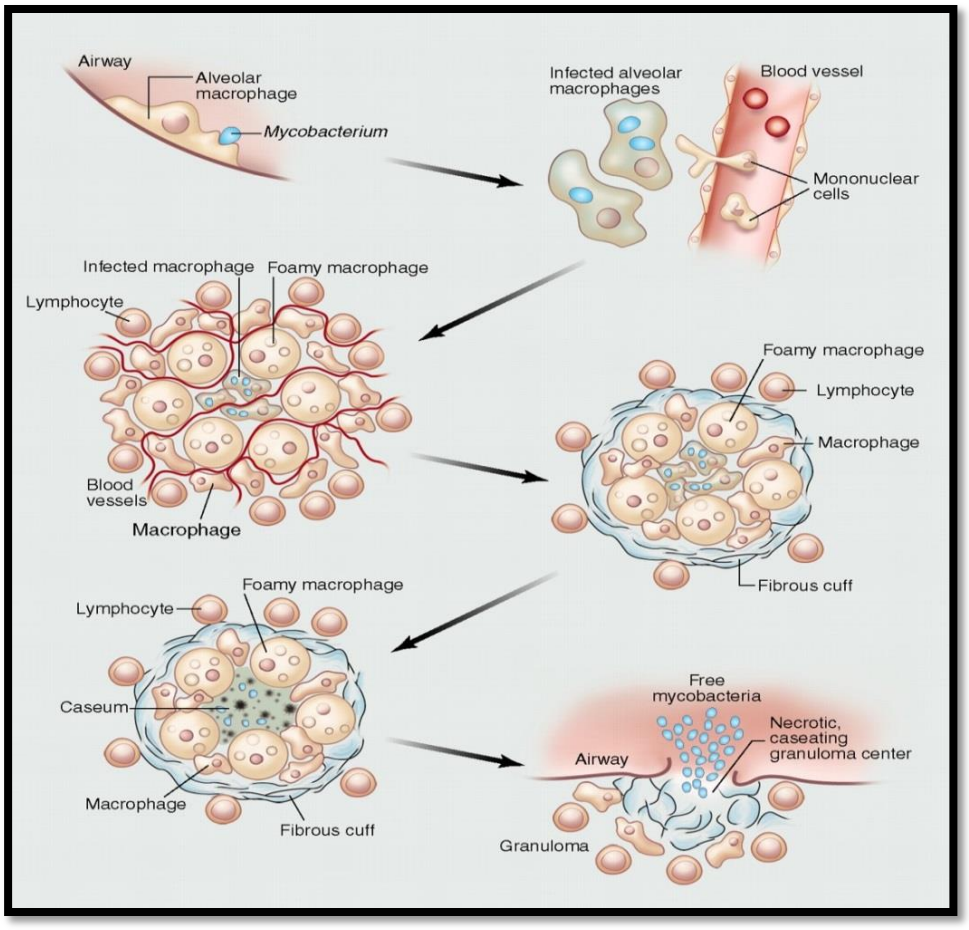

Figure 1: The life cycle of *M.tuberculosis*.

The figure shows the process of *M.tuberculosis* uptake followed by granuloma formation, granuloma caseation (accumulation of necrotic cell debris in the centre) and granuloma rupture [25].

1.3 The outcomes of initial infection with *Mycobacterium tuberculosis*

1.3.1 Primary progressive TB

Forty percent of infections progress towards primary active TB in which the immune system of the host is unable to subvert or contain the bacilli [26] (FIG.2). In this progressive form of TB, initial infection is followed by a gradual expansion of infected tissue that could result in the complete destruction of the infected organ [27]. When left untreated, the mortality rate of progressive TB is about 66% [6].

1.3.2 Latent TB

In the remaining 60%, TB will persist in a state of latency, a non-transmissible form in which clinical signs of disease are absent [28]. It is estimated that one third of the world's population carry this latent version of TB [7]. The majority of this group will live their lives without ever knowing that they carry the disease, but some (2-23% lifetime risk) will experience reactivation of the infection to secondary active TB. For people with compromised immunity, i.e. because of HIV/AIDS or the use of immuno-supressing drugs, the numbers are much higher (5-10% annual risk) [29].

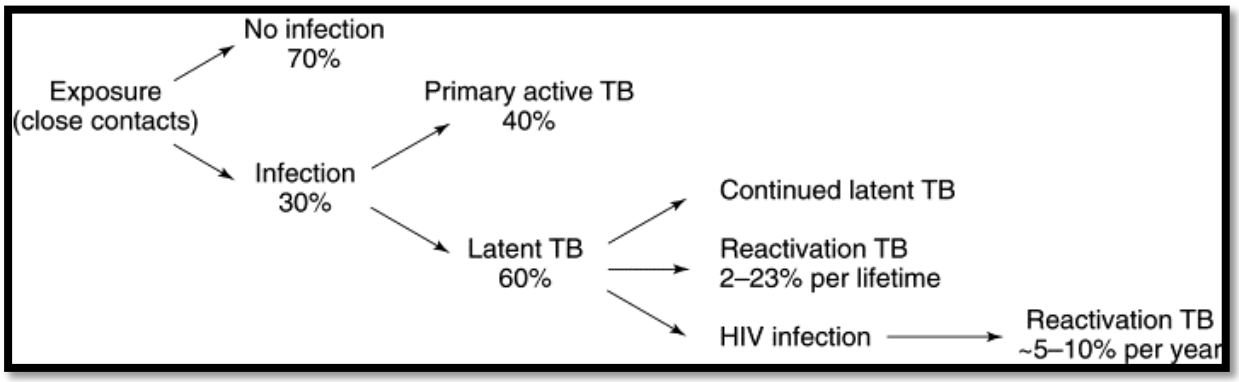

Figure 2: Outcomes associated with exposure to Mycobacterium Tuberculosis [26].

1.4 The granuloma

In mice, TB-specific lymphocytes can be detected 2-3 weeks post-infection [28]. Their appearance mark the onset of a "containment"-state wherein the bacterial burden remains relatively constant [30]. T- and B-lymphocytes migrate to and associate with the periphery of the developing granulomas. The classic TB granuloma is highly vascularized, with infected macrophages in the centre. These are surrounded by other macrophages that differentiate into several different morphotypes; epitheloid macrophages, giant multinucleated macrophages and foamy, lipid-filled macrophages [25] (FIG.1). Towards the periphery of the granuloma one finds fibroblasts, which synthesize a fibrous cuff that encloses the central structures, and excludes the majority of lymphocytes from the core of the granuloma [31]. It was a long held view that granuloma formation was purely a host defensive mechanism. By constructing a static and impermeable barrier around the foci of bacterial growth, the granulomas were believed to thwart and contain the infection [32]. However, studies by Ramakrishnan et.al have shown that superinfected mycobacteria rapidly traffic into pre-existing granulomas in the zebrafish model, indicating that the granulomas are more dynamic than once believed. Another crucial finding was that macrophages, although they are important in curtailing bacterial growth, may be unwitting accomplices in the spread of the bacilli during early stages of infection [33, 34]. In progressive forms of TB, granuloma centers become less vascularized causing hypoxia and caseating necrosis (caseum=cheese, refers to the cheese-like substance that consists of liquefied, necrotic cell debris in the granuloma core) [35]. Ultimately the granuloma ruptures, spilling thousands of viable bacilli into the airways. This leads to coughing and the release of aerosolized bacilli that may infect a new host [36]. A granuloma may also rupture into a blood vessel and cause the miliary tuberculosis described previously[27].

1.5 Why we have failed to eradicate the disease?

1.5.1 Failure of our own immune system

Only about thirty percent of those who have been exposed to the TB bacilli will contract the disease [26]. So under normal circumstances our immune system is successful in its attempt to clear the pathogen. The macrophages will internalize the bacilli and sequentially fuse the phagosome with early and late endocytic organelles and become phagolysosomes. The

tubercle bacillus however has the ability to arrest phagosomal maturation and prevent phagolysosomal fusion [37](FIG.3). It is this ability that is most widely attributed the tubercle bacilli's enhanced survivability inside the macrophage, as it allows them to avoid the bactericidal environment of the phagolysosome. *M.tuberculosis*-containing phagosomes fail to acidify [38] and fail to acquire mature lysosomal hydrolases [39], while they retain access to recycling endosomes that can provide crucial nutrients, such as iron, to the pathogen [31]. Several mechanisms have been implicated in this phagosomal maturation arrest, for instance; inhibition of calcium transients prior to phagosome fusion [40], altered lipid and protein composition of the phagosome preventing assembly of factors that control fusion events [41, 42], inhibition of actin assembly by phagosomes [43] and interference with the Rab-controlled trafficking system [44]. The mechanisms underlying this pathogen survival-strategy are probably multi-factorial, but they remain poorly understood. Some reports suggest that the bacilli can inhibit MHC class II processing and presentation, thereby preventing the recognition of infected macrophages by $CD4^+$ T cells [45]. Immunoglobulin-coating of the pathogen and exposing macrophages to interferon gamma (IFNγ) increases the chance that the pathogen will be sequestered into phagolysosomes [46, 47], so a competent immune system is still critical in fighting the infection even if the pathogen may have evolved strategies for evasion.

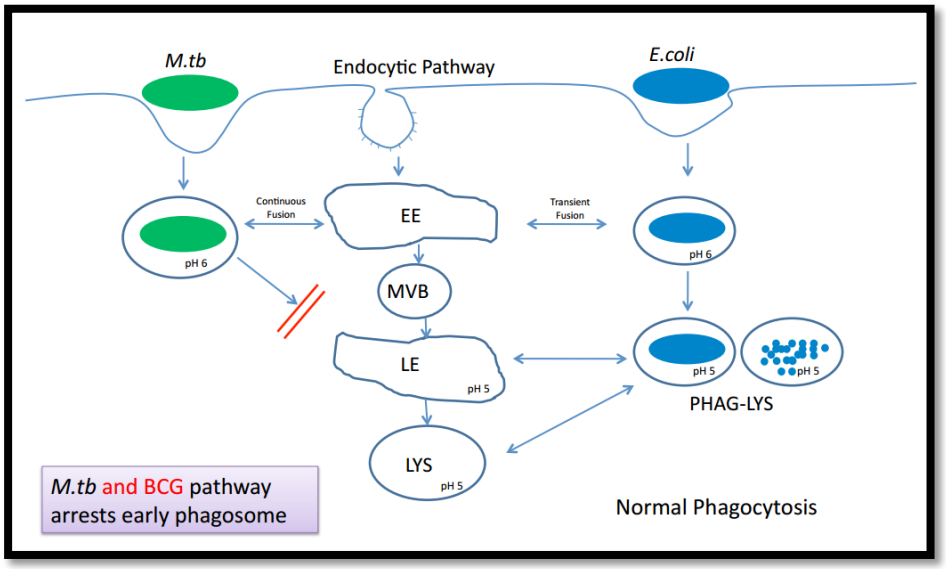

Figure 3: *M.tuberculosis* prevents phagosomal maturation

Shows how phagosomes containing none-pathogenic *E.coli* mature and fuse with an acidic lysosome resulting in the destruction of the bacterium. Phagosomes containing *M.tuberculosis* (or BCG) are prevented from maturing and fusing with the lysosome. As a consequence the pathogen is not destroyed (courtesy of G.Griffiths).

1.5.2 Failure of the medical/research community

One might also ask why we, as a research/medical community, have failed to eradicate the disease. The question should be even more imposing when we know that we have a vaccine and effective chemotherapeutic agents at our disposal. Some of the problems with the current chemotherapy are already highlighted. Problems with chemotherapy-treatment are confounded by the fact that the pathogen has a nearly impenetrable cell membrane [48] and has the ability to up-regulate efflux pumps that can expel intracellular drugs [49]. The emergence of multidrug resistant strains of the tubercle bacilli (MDR-TB), which accounted for 3.7% of all new cases and 20% of all previously treated cases in 2012 [6], should provide additional motivation to develop new medicine. In addition, it has proven difficult to develop a vaccine that provides lifelong protection against the disease. This is much down to the fact that an individual is susceptible to reinfection even after a natural primary infection and clearance [50]. The current vaccine, Bacillus Calmette-Guèrin or BCG, seems to be partly effective in some parts of the world [51] but not in others [52]. A reason for this discrepancy might be attenuation of the vaccine because of serial passages or other preparation methods, making the vaccine become too benign to elicit an adaptive immune response [53]. Another explanation could be induction of tolerance to BCG after contact with environmental mycobacteria [54]. Although development of more effective vaccines is desirable, it is important to add that even if we gave to every human being, a vaccine that effectively blocked all transmission of the disease we could still expect several hundred millions new cases of active TB due to reactivation of latent infections.

1.6 Introducing nanobead-based interventions for treatment of tuberculosis

Several groups have introduced the interesting concept of using nanoparticles (NPs) in TB therapy. The basic idea is to encapsulate anti-tubercular drugs inside a biodegradable polymer. When administered to the patient the desired effects are as follows: the gradual breakdown of the matrix should lead to gradual release of encapsulated drug, the matrix should protect the drug against enzymatic breakdown thus prolonging its residence time in the patient and the increased size of the construct should exceed the renal threshold thus avoid kidney filtering and again, prolonging residence time. These traits are desirable for many drugs aimed at clearing many different infections. There could also be one specific advantage

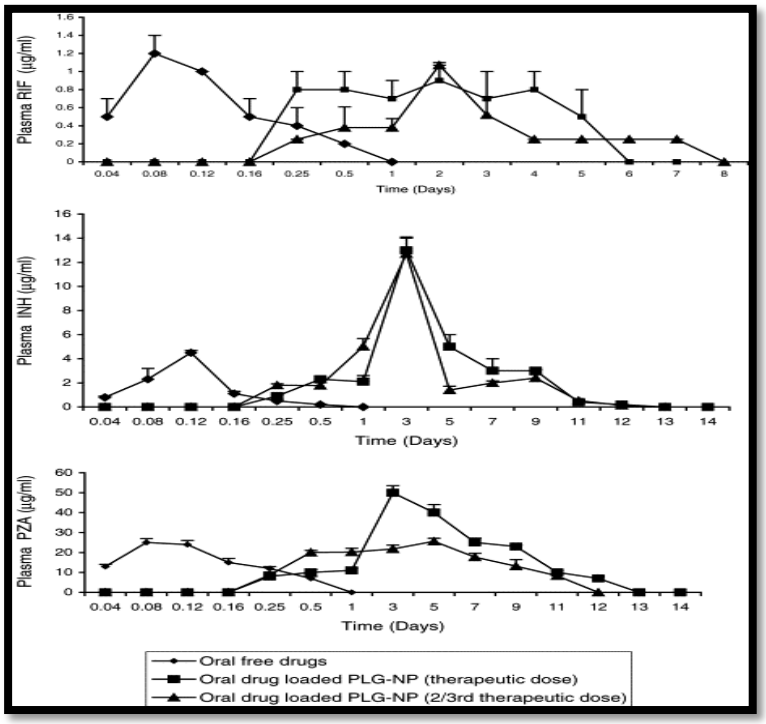

Figure 4: Nanobeads encapsulating drug have longer residence time compared to free drug

Plasma drug levels following a single oral administration of three frontline anti-TB drugs rifampicin (RIF), isoniazid (INH) and pyrazinamide (PZA) to guinea pigs. Results are mean ± SD, *n* = 5-6 [55].

	Log CFU/ml homogenate	
Groups	Lung	Spleen
Untreated controls	5.44±0.38	5.16± 0.36
Empty PLG-NP every 10 (5 oral doses)	4.62±0.28	4.66± 0.31
Oral free drugs at 2/3 therapeutic dose (46 daily doses)	4.26±0.41	4.15± 0.32
Oral free drugs at therapeutic dose (46 daily doses)	< 1	< 1
Drug loaded PLG-NP at therapeutic dose every 10 days (5 oral doses)	< 1	< 1
Drug loaded PLG-NP at 2/3rd therapeutic dose every 10 days (5 oral doses)	< 1	< 1

Table 1: Therapeutic effect of nanobeads loaded with rifampicin

The table shows the therapeutic effect of PLGA nanoparticles loaded with rifampicin compared to the same amount of free rifampicin in treating guinea-pig infected with *M.tuberculosis*. Results are based on visible growth of *M.tuberculosis* on 7H10 agar 21 days post-infection. Results show mean ± SD, *n* = 5-6 [55].

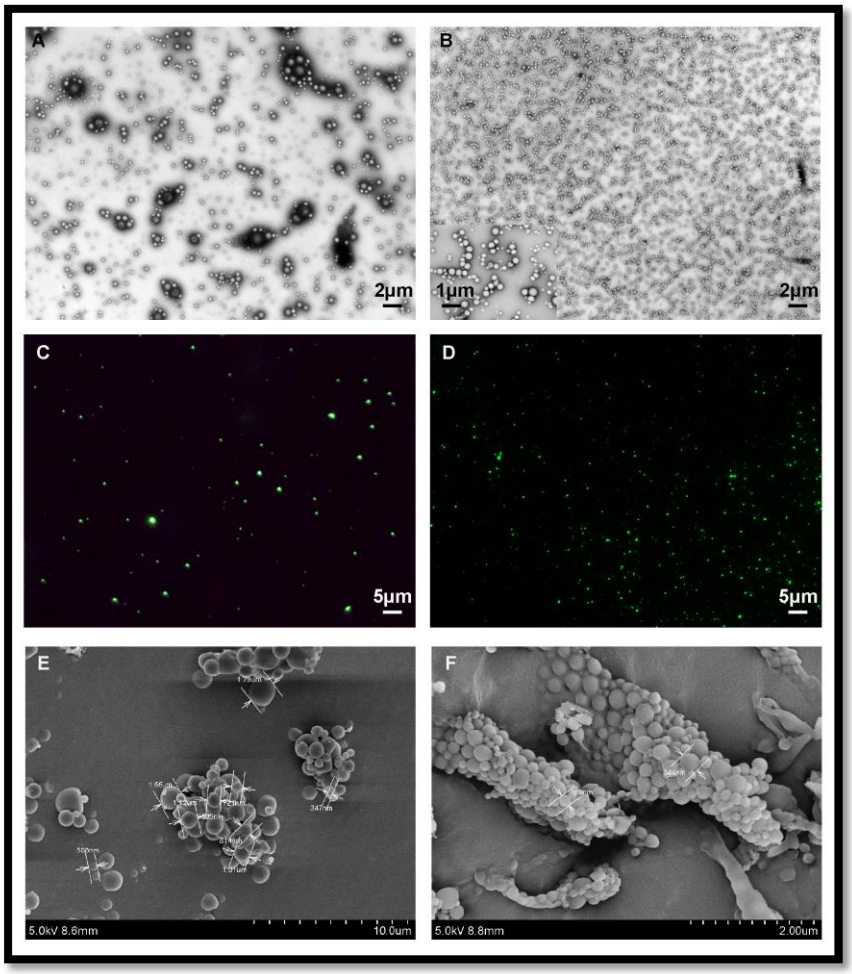

Figure 5: Microscopy of Nanoparticles.

Images obtained using TEM (A and B), confocal microscopy (C and D) and SEM (E and F). A, C and E show NPs made with the standard preparation method while B, D and F show the NPs prepared after selective centrifugation [56].

to encapsulating drugs aimed at clearing granulomatous diseases. Phagocytic cells can ingest particles with diameter sizes ranging from 100nm to 10µM [57]. This is an attractive scenario since the tubercle bacilli reside mainly in professional phagocytes, namely macrophages. Not only do the macrophages harbor the bacilli, but they are actively recruited to the developing granulomas, the foci of bacterial growth [17]. A desired effect of treating TB with nanobeads is thus a natural co-localization between the drug and the pathogen. Prof.Gopal Khuller and his collaborators have pioneered work on nanobead-based interventions for treating TB. In a series of papers his group convincingly demonstrates the effects of encapsulated anti-TB drugs on gradual release, prolonged residence time and improved therapeutic effect in the

mouse and guinea pig models [55, 58-61] (FIG.4 and TABLE.1). In collaboration with the Khuller group and polymer chemists from Professor Bo Nystrom's group at UiO, Federico Fenaroli has succeeded in making PLGA nanoparticles encapsulating rifampicin (RIF), one of 4 frontline anti-TB drugs, of sizes ranging from 50nm to 2μM (FIG.5) and drug loading around 34% (w/w). RIF exerts its bactericidal effect by binding to the DNA-dependent RNA-polymerase thereby blocking transcription [62]. PLGA has been our preferred choice of polymer due to its biodegradability and biocompatibility [63]. Other polymers such as chitosan [64] and alginate [65] have been explored as alternatives to PLGA, but we have had best results using PLGA. These NPs can be administered to mammalian models through the oral-, inhalation- or intravenous route [55]. The main focus of my work has been to evaluate the effect of these nanoparticles in treating zebrafish larvae challenged with mycobacterial infection.

1.7 Experimental models of TB pathogenesis

Many discoveries about the pathogenesis of mycobacteria have been made using cultured cells [66]. Drosophila and Dictyostelium have been used to elucidate host-pathogen interactions during early infection [67, 68], but to understand the complexity of the events leading to granuloma formation and disease states, vertebrate models are needed. The animal model that most closely recapitulates the progression of human TB is the macaque [69]. However due to cost and ethical considerations the use of this model has been limited. Rodent models have been instrumental in unveiling facts about the pathogenesis of TB [70]. They do however have their own idiosyncrasies that make them less than perfect models for all aspects of human TB. Mice, the most commonly used mode of TB, form poorly organized macrophage and lymphocyte aggregates that do not caseate [30]. Guinea-pigs are exquisitely susceptible to a progressive pulmonary infection [71], while most rabbits are resistant to *M.tuberculosis* [72]. We have been inspired by the group of Lalita Ramakrishnan at the University of Washington (Seattle, USA) and employed the zebrafish as our model organism for unveiling novel aspects about nanobead-based therapies of TB [73]. The key advantage for our research is that the zebrafish embryos are transparent, allowing us to perform optical measurements which would be impossible on other model organisms.

1.8 The zebrafish (Danio rerio) as a vertebrate model organism to study TB

From being an aquarium fish that was occasionally studied in the laboratory in the 1960's [74], the zebrafish has risen to prominence and become a complement and an alternative to the mouse model for biomedical research. This fish is an excellent laboratory animal for several reasons; they are small, robust, inexpensive to maintain and have well-defined husbandry standards. Embryo development is well characterized and the genome is fully sequenced [75-78]. Teleost fish have both an innate and adaptive immune system, with conserved orthologues of key human and mouse immune genes [79], including a broad range of Toll-like receptors (TLRs) and complement factors [80, 81]. Upon mycobacterial infection, the zebrafish develops organized, caseating granulomas reminiscent of human TB albeit with fewer lymphocytes [82]. The lymphocytes remain functionally important in curtailing bacterial growth since rag1-deficient adult zebrafish (that lack T- and B-cells) are hyper-susceptible to mycobacterial infection, similar to rag1-deficient mice [73, 83]. Precursor lymphocytes can be detected just 3 days post- fertilization (DPF) but they are not fully functional until 3 weeks later [84]. Macrophages on the other hand, are able to kill non-pathogenic bacteria just 1 DPF, while the first neutrophils can be detected 2 DPF [79]. This means that there is a window of almost 3 weeks in which we can study the exclusive contribution of innate immunity to combat bacterial infection. This makes the zebrafish an ideal model for investigating the initial events of TB-pathogenesis, from early infection to granuloma formation.

Fertilized zebrafish embryos are kept at 28 ˚C. This is a non-permissive temperature for *M. tuberculosis* growth. We therefore use a close relative of *M.tuberculosis*, namely *Mycobacterium marinum*, as a model for TB in the zebrafish embryo.

1.9 *Mycobacterium marinum*

Mycobacterium marinum is a macrophage pathogen that causes a systemic, granulomatous disease in ectotherms [85]. In contrast to *M.tuberculosis*, which is transmitted almost exclusively from lung to lung, *M.marinum* inhabits marine and freshwater reservoirs [86]. It grows optimally at 25-35 ˚C so manifestation of human infection is primarily limited to the extremities [87]. This species of Mycobacterium was originally isolated in Sweden in 1951

[88] and phylogenetic studies later revealed its close relation to *M.tuberculosis* [89] (FIG.6). A framework of pathogenesis seems to be conserved between the two species. They both survive inside macrophages by arresting phagosomal maturation, they induce similar initial host response to infection with elevated expression of TNFα and IL-1β and they both extravasate into tissue to form granulomas [90, 91]. The *M.marinum* genome is 85% identical to orthologous regions of the *M.tuberculosis* genome, and coding sequence amino acid identity averages 85% between orthologues. At 6.6Mb the *M.marinum* genome is about 1.5 times the size of the *M.tuberculosis* genome, perhaps reflecting its expanded environmental host range [92]. Mutational analyses into the 2.2Mb that is unique to *M.marinum* and the 0.6Mb that is unique to *M.tuberculosis*, have yielded very few virulence phenotypes [93, 94]. Furthermore, immunization with *M.marinum* has been shown to provide protection against *M.tuberculosis* in the mouse model [95].

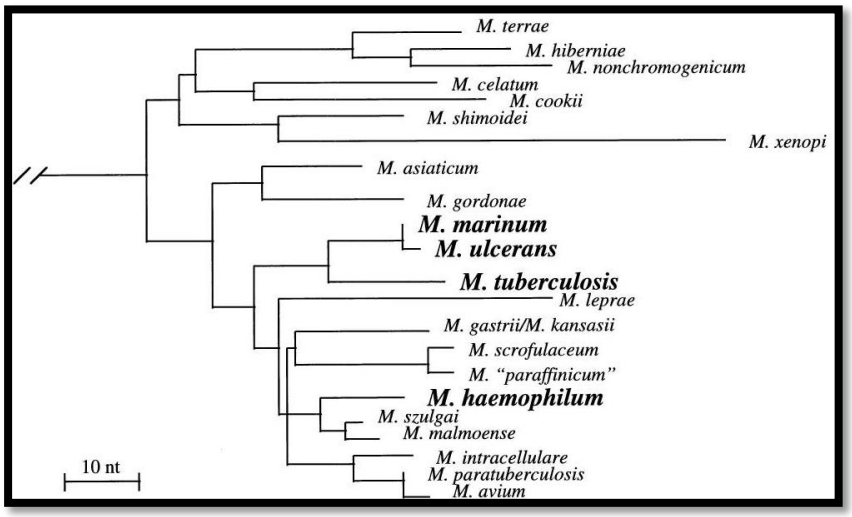

Figure 6: Phylogenetic tree showing the close genetic relation between *M.marinum* and *M.tuberculosis*

Phylogenetic tree based on the alignment of partial 16S rRNA gene sequences illustrating the positions of strains of *M.ulcerans, M.marinum, M.tuberculosis* and *M.haemophilum* and other slowly growing mycobacterieal species. The tree was rooted by use of *N.asteroides* as an outgroup. The bar indicates a 10-nucleaotide (10-nt) difference [89].

Prof. Astrid van der Sar of Vrije Universiteit Medical Center, The Netherlands, has proposed a division of *M.marinum*-strains based on genetic diversity and virulence in the adult zebrafish; the M-strains which are extremely virulent in the adult zebrafish and most often isolated from human infections, and the E-strains which are less virulent in the adult zebrafish and most often isolated from environmental reservoirs [96, 97]. In the beginning of

my master thesis project, I wanted to characterize the virulence of this E-strain *M.marinum* in the zebrafish larvae. A less virulent strain of *M.marinum* could increase the time-frame in which we can perform measurements in the young larvae, a seriously limiting factor for some experiments.

2 Aims

I will show in the Results-section how the M-strain of *M.marinum* causes a systemic and lethal disease in the zebrafish larvae. When untreated, the mortality rates have been around 60% just ten days post-infection. This has left us with very little time in which to perform measurements of the developing infection. As already mentioned, less virulent strains of *M.marinum* have already been used to unveil facts about TB in the adult zebrafish [96, 97].

- In the beginning of my master thesis project, I therefore sought to evaluate the virulence of the E-strain *M.marinum* (E11) in the zebrafish larvae. The use of this presumptive less virulent strain could increase the resolution of our experiments. This experiment could also form the basis for studying genetic components of mycobacterial virulence.

When I first started my master thesis, CFU (Colony Forming Units) was the standard method for estimating bacterial burden of the zebrafish larvae in our group. Unfortunately there were some disadvantages with this method; it has a low throughput, it is labor intensive and since the procedure demands that we kill the larvae, huge test groups were required to obtain solid statistical data. Furthermore, the results obtained from using this method have proven to be unreliable, especially in the early stages of infection when bacterial burden can be low. In addition it soon became apparent that the two most prominent groups working on *M.marinum* in zebrafish (Ramakrishnan and Meijer) gave up trying to use CFU analysis and both switched to estimating the level of bacterial fluorescence

- The main goal of my thesis has therefore been to develop and apply a method for measuring the therapeutic effect of NP-treatment of tuberculosis in the zebrafish larval model. The method is called fluorescent pixel count (FPC) and is made possible by infecting the transparent zebrafish embryo with *M.marinum* that carries a fluorescent marker.

3 Methods

3.1 Zebrafish breeding and maintenance

From Darren Gilmour at EMBL (Heidelberg, Germany), we received ~100 Nacre -/- strain embryos that were grown to adulthood by Jan-Roger Torp in Peter Aleström's zebrafish facility at the Norwegian School of veterinary Science. The Nacre strain is transparent from embryo until adulthood. Some of the adult fish were later transferred to our facility at the UiO where they are now kept at 28ºC in well-aerated tanks. Approximately 10% of the tank water is replaced every day by fresh system water and the light cycle is 12:12 hrs. The fish are fed 3 times per day, once with SDS 400 dry food (Lillicotech) and twice with brine shrimp. The zebrafish can breed every two weeks. On the day before breeding 3 males and 2 females are placed in a tank separated by a splitter. The bottom of the tank is filled with marbles to keep the fish from eating the eggs. The zebrafish breed at dawn and so in the morning before the light cycle begins, the splitter is removed to allow the males access to the females. Once the light cycles has begun the spawning goes on for ~2 hrs after which we can collect the fertilized eggs. The embryos are transferred to sterile embryo medium (see recipe) and kept at 28ºC until they are dechorionated ~30 hrs post-fertilization.

3.2 Preparation of PLGA nanoparticles enclosing the drug rifampicin

Adapted from Kalluru 2013 [56].

Materials

PLGA (Poly (D,L)-lactide-co-glycolide) 50:50 RESOMER® RG 502 (Evonik Röhm Gmbh)

Polyvinyl alcohol (PVA) (Alfa Aesar)

Rifampicin (RIF) (Sigma-Aldrich)

Dichloromethane (DCM) (Sigma-Aldrich)

Coumarin-6 (Aldrich)

Mannitol (Sigma-Aldrich)

Procedure

An oil-in-water emulsion (O/W) using the solvent evaporation method was used as our standard procedure to prepare rifampicin loaded nanoparticles. Rifampicin (100mg) and PLGA (100mg) were dissolved in 10 ml DCM, with or without 0.2 mg of coumarin-6 and stirred overnight at room temperature. For the water phase 200 mg of PVA was dissolved in 20 ml water (prefiltered using a 0.2 μm filter) with heating to 90ºC for 1hr and stirring vigorously with a magnetic stirrer overnight at room temperature. The two solutions were mixed and tip-sonicated (Sonics, Vibracell) for 3 minutes to obtain the emulsion. Subsequently, the emulsion was put in a flask and kept stirring, allowing complete evaporation of the DCM within 10-14 hours. For this, a piece of aluminum foil was applied on the top of the flask and punctured with a hole of about 0.5 cm diameter. Once the evaporation step was completed, NPs were washed twice with water and collected via centrifugation at 8000 rpm for 20 min using a Beckman coulter 32 Ti rotor. Subsequently, they were re-suspended in a 0.5% mannitol solution, freeze-dried for 2 days and stored at 4ºC.

3.3 Preparation of *M.marinum* stocks for infection of zebrafish embryos

Adapted from Cosma et.al 2006 [98]

Materials

7H9 liquid culture medium (see appendix - recipes)

ADC (see appendix - recipes)

20% (v/v) Tween 80 (Sigma-Aldrich)

PBS with 2% (w/v) polyvinylpyrrilidone (PVP) (Merck)

M.marinum frozen stock or bacterial colony of either the M- or the E-strain (see appendix – bacterial strains)

Kanamycin (Sigma-Aldrich) or Hygromycin (Sigma-Aldrich)

33˚C incubator

Procedure

2mL of ADC and 50µL of 20% (v/v) Tween 80 was added to 18 mL of 7H9 liquid culture medium. 16 µL of 50mg/mL kanamycin or 20µL of 50mg/mL hygromycin was added for the M- and the E-strain respectively. The medium was subsequently inoculated with a small scraping of bacterial colony or *M.marinum* frozen stock. The flasks were then incubated at 33ºC until it reached log-phase growth that is an OD_{600} between 0.3 and 1.2 (may take several days depending on you starting bacterial concentration). To measure the OD_{600}, 1.5mL of the inoculum was pipetted into a microcentrifuge tube, and spun at maximum speed in a microcentrifuge. The supernatant was replaced with 2% PVP in PBS. The solution was then passed through a 27g needle repeatedly until it was well dispersed, then loaded into a polystyrene cuvette for OD_{600}-measurement. The measurement was performed by using an Eppendorf Biophotometer and we confirmed that the OD_{600} was within log-phase range.

3.4 Injection of zebrafish embryos with *M.marinum*, PLGA-RIF nanoparticles or free RIF by microinjection

Adapted from Cosma et.al 2006 [98]

Materials

M.marinum in log phase growth in 2% (w/v) PVP (Merck) in PBS (see protocol) or PLGA nanoparticles in 2% (w/v) PVP in PBS

Zebrafish embryo medium (see appendix - recipes)

2% (w/v) phenol red (Sigma-Aldrich) for visualization

Tricaine stock solution (see appendix – recipes)

2% (w/v) agarose plates

Dechorionated zebrafish embryos 48hrs post-fertilization

Borosilicate capillaries (SM100F10-Harvard Apparatus)

Micropipette-puller (Sutter P-97)

Mineral oil (Sigma-Aldrich)

Glass slide with a 0.1mm ruler (Leica)

Micromanipulator (Narishige MN150)

Microinjector (Eppendorf Femtojet)

Jeweller's forceps (Dumont No.5)

Water bath ultrasonicator (Merck)

Procedure

Preparing the needle for injection

Bacteria were prepared for injection as described in previous protocol and phenol red was added to a final concentration of 0.2% (v/v). By using a micropipettor with a microloader tip, 5 µL bacterial suspension was drawn up to fill the injection needle (needles were pulled with the following settings: Heat=610, Pull=40, Velocity=80, Time=5). The injection needle was mounted to the microinjector/micromanipulator and positioned at the microscope where the injection would take place. A droplet of mineral oil was added to a glass slide with a 0.1mm-ruler and placed underneath the needle tip. The tip of the needle was subsequently immersed in the oil and broken off with a pair of jeweller's forceps. The solution was injected into the oil and the diameter of the droplet, visible because of the phenol red, was measured against the ruler underneath. By using the forceps, enough of the needle tip was broken to obtain a droplet of the desired size. The size of the droplet was also regulated by adjusting pressure and ejection time on the microinjector.

Preparing embryos for injection

A small number (2-10 depending on operator speed) of dechorionated embryos, were transferred to a small petri dish with sterile embryo medium and tricaine stock solution (300µL tricaine stock solution added to 4.7 mL embryo medium) and left for at least 2 min for

full anaesthesia. The embryos were transferred to a 2% agarose plate, excess liquid was removed and the embryos positioned so that the needle pointed towards the intended injection target.

Infecting embryos with bacterial suspension

The fish was penetrated such that the needle tip was positioned inside the intended injection target (for different injection targets see figure 6). Injection pressure was applied to drive the bacterial suspension into the fish.

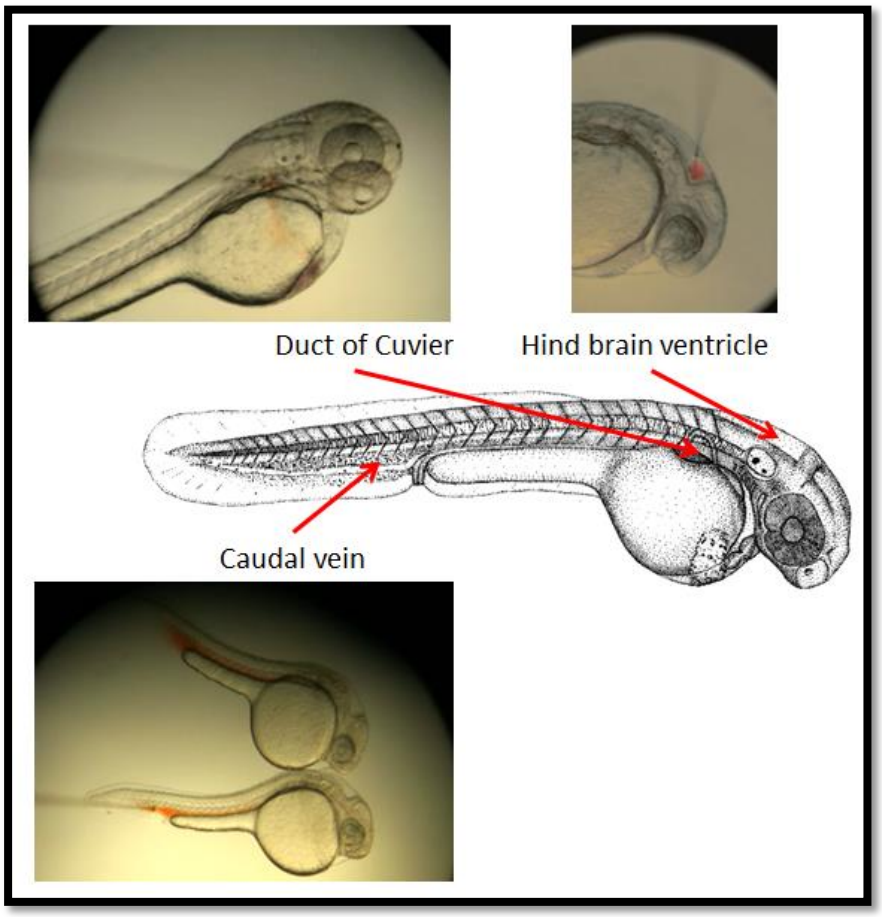

Figure 6: Different injections targets

Injections of phenol red dye into the Duct of Cuvier, hindbrain ventricle and the caudal vein at 48hr post-fertilization [99].

Injecting embryos with PLGA nanoparticles

The method is very similar to injection of bacterial suspension. The bacterial suspension was replaced by PLGA nanoparticle suspension - which is the desired amount of PLGA nanoparticles in 2% PVP in PBS with 0.2% Phenol red. The tube containing the PLGA nanoparticle suspension was placed in a water bath ultrasonicator for 5 min before the solution was loaded into the injection needle.

Injecting embryos with free rifampicin

The drug was solubilized in 5% DMSO in PBS before the solution is loaded into the injection needle. It was not possible to solubilize PLGA nanoparticles in DMSO as it would dissolve the beads.

3.5 CFU enumeration from zebrafish larvae

Adapted from Cosma et.al 2006 [98].

Materials

Zebrafish embryo medium (see appendix - recipes) supplemented with 20 µg/mL kanamycin (Sigma-Aldrich)

Zebrafish embryo medium (see appendix - recipes) supplemented with 200 µg/mL tricaine (Argent Laboratories)

Infected larvae (see method 3.4)

Trypsin-EDTA (Sigma-Aldrich)

PBS

1% (v/v) Triton X-100 (Sigma-Aldrich)

7H10 agar (see appendix recipes) plates with antimicrobial agents (see appendix - recipes, supplements to 7H10)

Procedure

500 µL sterile zebrafish embryo medium supplemented with 20 µg/mL kanamycin was pipetted into 2mL micro-centrifuge tubes. One tube was prepared for each larva to be lysed. One infected larva was transferred into each tube. Larvae were allowed to soak for 1 hr at room temperature. Most of the embryo medium was removed with a pipette tip while care was taken that the larvae remained in the tube. 500 µL of zebrafish embryo medium with 200 µg/mL tricaine was added, and the tubes were placed on ice for 1hr. The tricaine solution was removed and then replaced by 150 µL of 1 x trypsin-EDTA. Samples were then incubated for 1 hr at 30˚C. The tubes were then vortexed on maximum settings for 2 min and micro-centrifuged briefly at maximum speed to ensure that all the liquid was returned to the bottom of the tube. The tubes were subsequently returned to 30˚C. The samples were then vortexed every hour until there were no visible signs of larval debris (~4-5 hrs). When embryo digestion was complete, 30 µL PBS and 20 µL of 1% Triton X-100 was added to each tube and vortexed for 2 min Samples were then placed in a water bath ultrasonicator for 10 min and micro-centrifuged to consolidate the liquid. The entire volume was then pipetted onto 7H10 agar plates (with antimicrobial agents) and spread evenly. The plates were incubated at 33˚C until colonies could be counted (~4-5 weeks).

3.6 Determining bacterial burden in zebrafish using fluorescent pixel count (FPC)

Materials

An image processing package (Fiji® [100])

2% agarose plates

Sterile embryo medium (see appendix - recipe)

Tricaine stock solution (see appendix - recipe)

Zebrafish larvae infected with *M.marinum* carrying a DSred fluorescent marker (see method 3.4)

Procedure

Imaging the larvae

The larvae were transferred to a small petri dish with embryo medium and tricaine stock solution (150 µL tricaine stock solution was added to 4.85 mL embryo medium) and left for at least 30sec for adequate anesthesia. The larvae were then transferred to a 2% agarose plate and placed under a fluorescence microscope (Leica Fluorescence Stereomicroscope model M205 FA, with Leica DFC 365 FX Monochrome Digital Camera and Leica Microsystems Type EL6000 external light source). It was decided that the spinal cord just posterior to the head region was an appropriate focal point (in the z-plane of the fish) and this was where every image was taken. Two images were taken of each fish, one in transmission light- and one in the fluorescent light channel. The fish was subsequently transferred to a 48-well plate with embryo medium.

Image processing

The pictures were processed with the Fiji® image processing package (the following steps are described exclusively for Fiji®). A Rolling ball background subtraction [101] was performed on every image, using a rolling ball radius that was at least the size of the largest object that was not a part of the background. Since this was not always possible a value was set where the aforementioned premise held for the vast majority of the images. This procedure was performed with the same rolling ball radius on all images. Next, an objects counter analysis [102] was performed. The threshold value was set between the lowest grey value of true signal (fluorescent *M.marinum*-signal) and highest value of background signal. Since this was not always possible, a threshold value was set where the aforementioned premise held for the vast majority of the images. The program was then set to display surface map and statistics. The surfaces were controlled to verify that they actually did represent true signals by comparing the objects map to the original transmission- and fluorescence images (the image-processing is depicted in FIG.7). The statistics were subsequently exported to an Excel spreadsheet. From the Excel spreadsheet a value for the sum of integrated densities (Int.Den) was determined. This is the fluorescent pixel count (FPC) of a particular zebrafish – the numerical value that is a measurement for bacterial burden in the infected zebrafish larva.

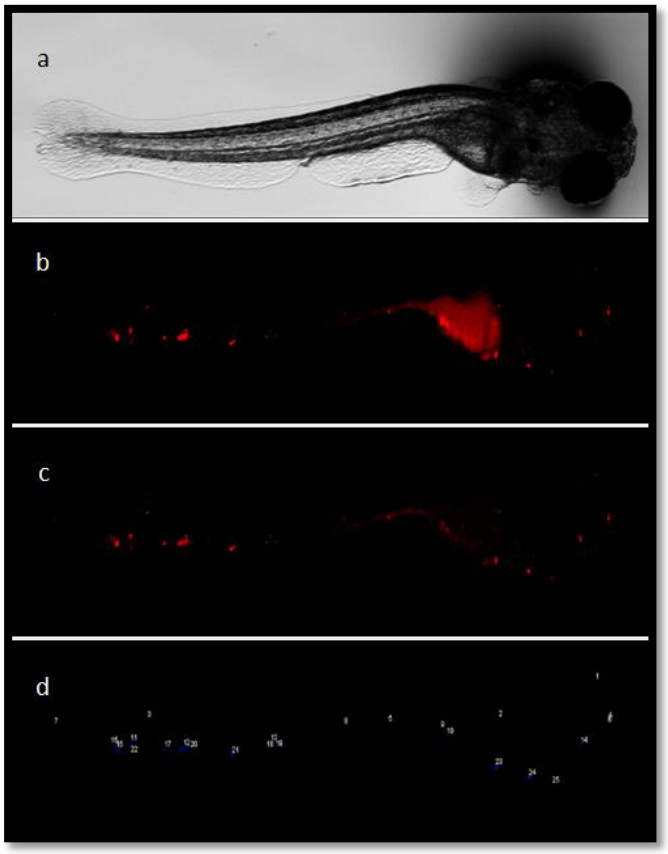

Figure 7: Images of the infected zebrafish as they are subjected to the FPC procedure.

Transmission image (a), fluorescence image (b), fluorescence image after rolling ball procedure (c) and surface map of objects found after thresholding (d) of a zebrafish larva infected with *M.marinum* then subjected to the FPC procedure.

4 Results

4.1 Establishing *M.marinum*-infection in the zebrafish embryo

Zebrafish embryos (Nacre -/-) were injected with 1nL *M.marinum*-solution of an OD_{600} of 0.9 into the caudal vein at 2dpf. Embryos were imaged the following day and then every second day over a 9-day period. Embryo water was replaced every day.

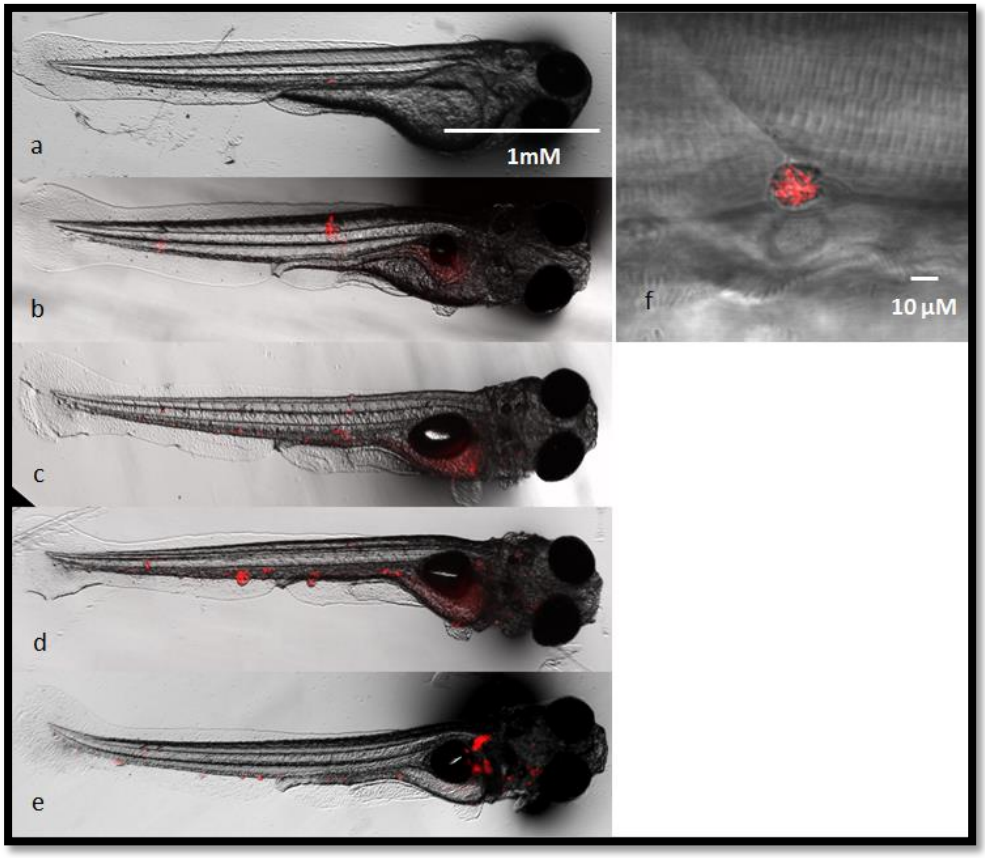

Figure 8: Images of one zebrafish infected with *M.marinum*.

A zebrafish infected with *M.marinum* 1,3,5,7 and 9 days post-infection (a, b, c, d and e respectively). All images are in-vivo merged transmission- and fluorescence images. Image f is a confocal image of a cluster of *M.marinum* inside an infected zebrafish larva. Images a-e were taken with a fluorescence stereomicroscope and image f was taken with an upright confocal laser scanning microscope.

Individual or small clusters of bacteria were detectable 1dpi. During the first days of infection, the bacteria seemed to colonize the tail rather than the head region. During the later

stages of infection, the head region was the one most heavily infected. It is not until 5-7dpi that big clusters of bacteria can be seen, presumably residing inside granulomas. Since they were not fed, uninfected larvae started to die from starvation around 10dpf. By this time about 60% of the infected larvae had died from *M.marinum*-infection.

4.2 E-strain vs. M-strain

4.2.1 Survival studies

Zebrafish embryos (Nacre -/-) were injected with either 1nL *M.marinum* M-strain solution of an OD_{600} of 0.9 or 1.2 nL *M.marinum* E-strain solution of an OD_{600} of 0.75 (= same number of bacteria) into the Duct of Cuvier at 2dpf. Embryo water was replaced every second day. The mortality rate of larvae infected with either the E- or the M-strain is used as an indication of the virulence of these two strains.

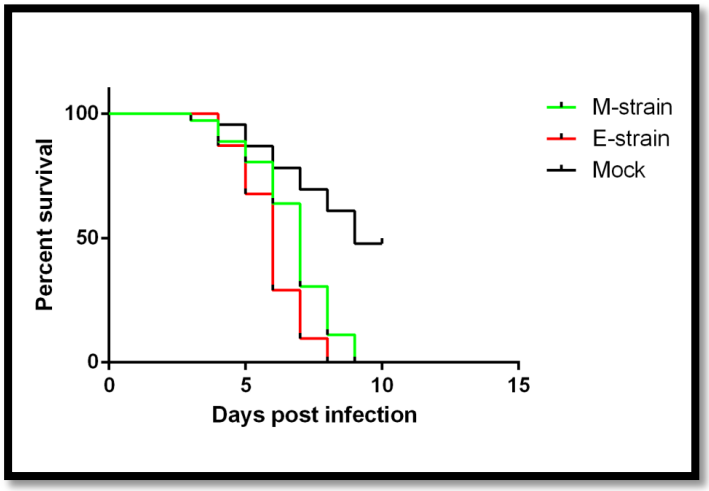

Figure 9: Survival of larvae injected with mock, E-strain and M-strain solution, experiment 1.

Cumulative mortality for larvae injected with PBS (mock), *M.marinum* E-strain and *M.marinum* M-strain. n≥23 for all groups

The mortalities of both *M.marinum*-strains compared to mock injection were deemed significantly different by a Log rank test. There was no significant difference in mortality between the two strains of *M.marinum*. The mortality of the uninfected group was high, possibly indicating that the batch of embryos used for this experiment was not in perfect health. Because of this, the experiment was repeated except injecting fewer bacteria (1 nL of OD_{600} of 0.36) of both strains and embryo water was replaced every day instead of every

second day. The results were similar - significant difference in mortalities between the mock- and the two *M.marinum*-injected embryos, but no difference between the mortalities of the two strains of *M.marinum*. These result differ from what was expected based on experiments performed on adult zebrafish [96, 97]. The M-strain-infected adult zebrafish had a significantly higher mortality rate than the E-strain-infected ones, but again, this effect was not seen in this zebrafish embryo experiment.

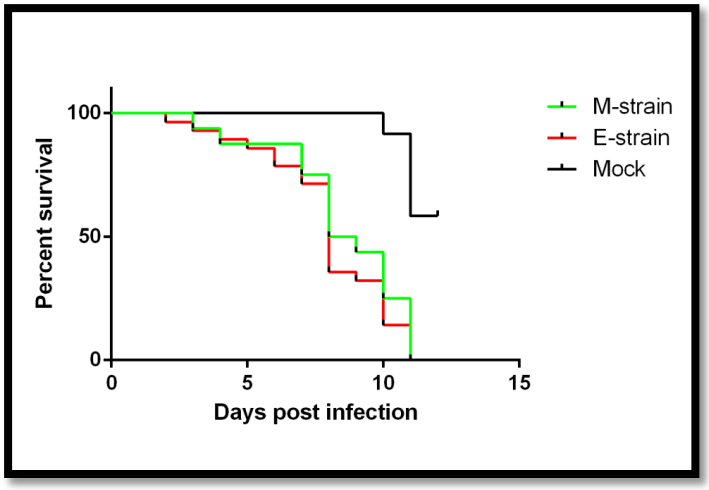

Figure 10: Survival of larvae injected with mock, E-strain and M-strain solution experiment 2.

Cumulative mortality for embryos injected with PBS (mock), *M.marinum* E-strain and *M.marinum* M-strain. n≥12 for all groups.

4.2.2 CFU enumeration of infected larvae

In addition to survival studies on the E- and the M-strain, a CFU procedure was performed (see 3.5). 5 larvae from each of the 3 groups were subjected to the CFU enumeration procedure at 2, 5 and 8 days post-infection

Days post infection	Mock	E-Strain	M-Strain
2dpi	0 ± 0	0 ± 0	0. ± 0
5dpi	0 ± 0	0.25 ± 0.5	0.6 ± 1.3
8dpi	0 ± 0	22.0 ± 23.5	10.2 ± 13.1

Figure 11: CFU-counts of the three groups (Mock-, E-Strain and M-Strain-injected embryos)

CFU counts in the three groups at three different time-points. Numbers are Mean±SD, n=5 in all groups.

In all groups the standard deviation was equal to- or higher than the average, possibly reflecting the variability with which individual zebrafish embryos respond to mycobacterial challenge. The results also reveal one of the shortcomings of the CFU method. In the fluorescence microscope we could clearly see bacteria inside the M- and the E-Strain-infected larvae at 2dpi. However, these bacteria could not be detected by the CFU method.

4.3 Problems of the CFU protocol

It might be possible to dissect the zebrafish larvae and isolate individual organs, but owing to their small size (~4mm length at 7dpf) we preferred to enumerate CFU from the whole animal. It is therefore necessary to prevent the outgrowth of the intestinal bacterial flora that might contaminate the growth medium. To counter this problem, a cocktail of 5 antibiotics to which the *M.marinum* is supposed to be naturally resistant (see recipe, supplement to 7H10 agar plates) was added to the solid medium on which we eventually plated our isolated bacteria. By plating diluted *M.marinum*-culture on these plates we sought to find out to what extent the heavy antibiotics pressure affected the growth rate of the bacilli. Bacterial cultures of ODs_{600} 0.2, 0.5 and 1.5 were diluted by 10^5. 100 µL of these suspensions were then plated on solid medium containing either no antibiotics, 1 antibiotic (kanamycin) or 5 antibiotics (see recipe, supplement to 7H10 agar plates). 9 technical replicas were made of each sample.

The results (FIG.12) show that the 5 antibiotics needed to prevent bacterial flora contamination also inhibit *M.marinum* growth. In fact, the CFU counts were ~3.5 times lower when using the plates containing 5 antibiotics compared to the plates without antibiotics. Furthermore, the colonies on the plates containing 5 antibiotics were visible after 31 days compared to only 10 days for the plates with no antibiotics. The 5-antibiotics cocktail consists of kanamycin to which this particular strain of *M.marinum* is resistant and 4 more antibiotics referred to as PACT (polymixin B sulphate, amphotericin B, carbenicillin and trimethoprim). The PACT-cocktail is a standard mix that is intended for the cultivation of mycobacterial species from specimens containing mixed flora [103]. Although several papers mention that the formulation might to some extent reduce the recovery of mycobacteria [104, 105], the extent to which it did so in our experiments came as a surprise. The CFU method was adapted from Cosma et.al 2006 [98] and results using this protocol on zebrafish larvae have been published in several prestigious journals [33, 91, 106].

No antibiotics *	Bacterial concentration (CFU/mL)
OD_{600} 0.2	1.13×10^7
OD_{600} 0.5	3.48×10^7
OD_{600} 1.5	7.61×10^7
Estimate for OD_{600} 1.0	5.89×10^7
Kanamycin *	
OD_{600} 0.2	0.94×10^7
OD_{600} 0.5	3.24×10^7
OD_{600} 1.5	6.94×10^7
Estimate for OD_{600} 1.0	5.27×10^7
5 Antibiotics **	
OD_{600} 0.2	0.04×10^7
OD_{600} 0.5	1.10×10^7
OD_{600} 1.5	4.00×10^7
Estimate for OD_{600} 1.0	1.70×10^7

* CFU were detectable after 10 days
** CFU were detectable after 31 days

Figure 12: CFU counts of 3 different concentrations of *M.marinum* plated on 3 different plates

3 different concentrations of *M.marinum* were plated on 3 different plates containing different antibiotics. The estimates for OD_{600} 1.0 are averages of each of the concentrations. n=9 in all groups (number of replicas)

4.4 Measuring the therapeutic effect of PLGA-nanoparticles encapsulating rifampicin in treatment of *M.marinum*-infection in the zebrafish larvae

4.4.1 Bacterial burden by FPC

Since the CFU procedure seemed unable to reliably quantify bacterial presence during early stages of infection and probably underestimated the bacterial burden during the whole period, I developed the FPC protocol described in the methods section (3.6). I subsequently applied this method to measure the bacterial burden in zebrafish larvae infected with 2nL of *M.marinum* suspension with OD_{600} 1.2 at 2dpf, then treated at 3dpf with 1; free rifampicin (12mg/kg tissue = 1xhuman dose) and 2; PLGA-nanoparticles encapsulating rifampicin (equal RIF-dose). The control groups were as follows: 1; uninfected larvae 2; infected but not treated larvae and 3; infected larvae then treated with empty PLGA-nanoparticles. All the

larvae were imaged just prior to drug treatment at 3dpf. The larvae were imaged again after 2, 4, 6 and 8days. The FPC value obtained from the images taken just prior to treatment at 3dpf represent initial bacterial burden (0dpt). Since the larvae displayed huge differences in initial response to *M.marinum*-challenge (FIG 13) it was decided that, when presenting the results, each time-point should represent change in bacterial burden from this day0-value. Embryo water was replaced every day.

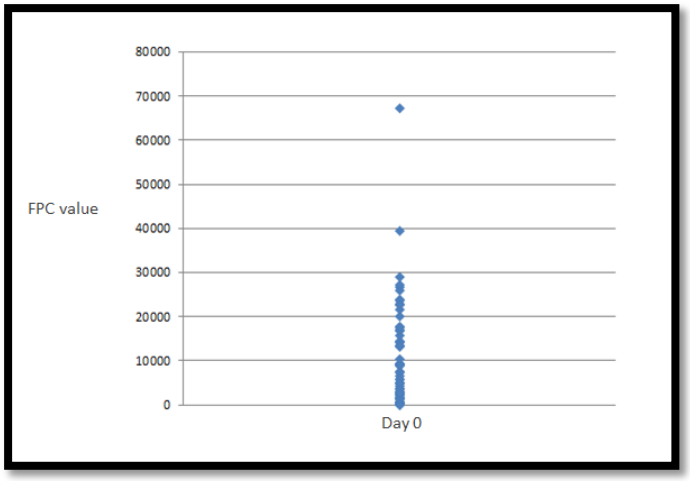

Figure 13: Zebrafish embryos respond differently to *M.marinum* infection.

Day0 represents 1 day post-infection. The figure shows that despite being injected with the same amount of bacteria, the zebrafish embryos have extremely variable levels of bacterial burden after one day. Each point indicates the estimate from individual embryos.

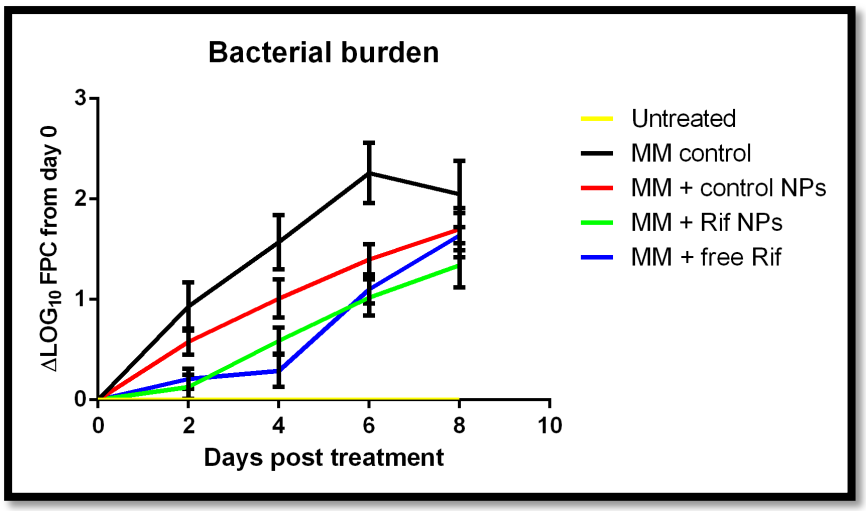

Figure 14: PLGA-RIF nanoparticle treatment of *M.marinum*-infected larvae results in a steady curtailment of bacterial growth.

Log_{10} FPC changes from day 0 for each of the 5 groups. Calculated as described in the Appendix. The lines represent Mean±SEM, n≥15 for all groups.

Bacterial burden of the larvae that are infected, but not treated is unsurprisingly the group that shows the most significant increase in fluorescence intensity throughout the surveillance period. The decrease in burden from day6-day8 in this group can be explained by the fact that 9 of the highly infected larvae died during this time-period. These larvae had average ΔLOG_{10} FPC values of around 3 at the time-point before they died ($=10^3$ increase in bacterial burden from day 0). This value can be viewed as the maximum bacterial growth that the larvae can sustain without dying. Both the rifampicin beads and the free rifampicin had a significant therapeutic effect throughout the surveillance period. The rifampicin beads-treated larvae had a lower bacterial burden at 8dpt compared to the free rifampicin-treated larvae, but the difference was deemed not significant (p-value = 26%). The same two groups show a biphasic growth curve although the phases change at different time-points. The big surprise of the experiment is still the effect of empty PLGA-beads which after 2dpt exhibited the same therapeutic effect as beads containing RIF.

4.4.2 Survival studies

The FPC method should have allowed us to perform a survival study on the same larvae. However, we needed to feed the larvae during the surveillance period in order to ensure that they died from infection rather than starvation. The SDS100 dry food (Lillicotech) is

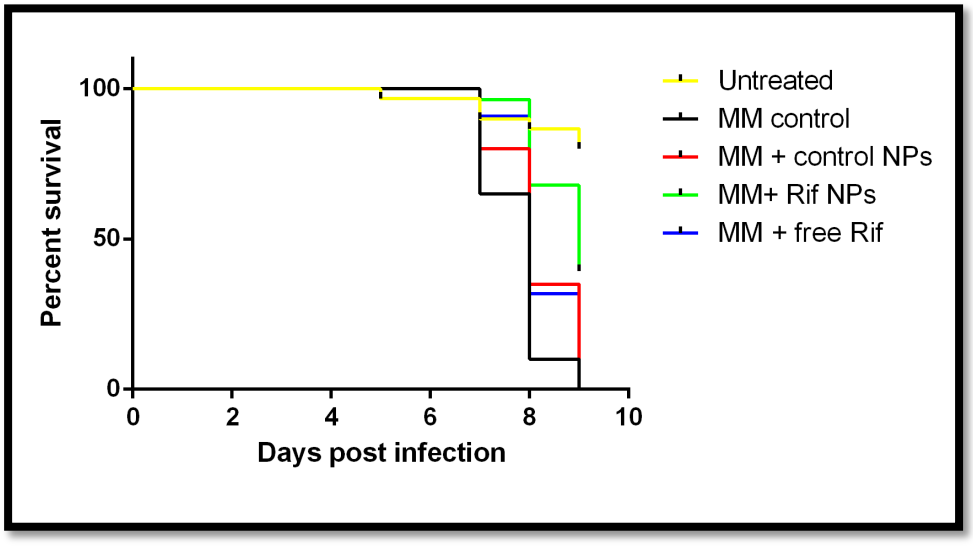

Figure 15: PLGA-RIF nanoparticle treatment significantly increases survival of *M.marinum*-infected larvae compared to free RIF

Cumulative mortality for each of the 5 groups of larvae. The experiment reveal a significant increase in survival of embryos treated with RIF NPs compared to free RIF. n≥15 for all groups.

unfortunately intensely fluorescent in both red and green channels and so we performed a survival experiment at a later time using the same 5 groups with exactly the same treatment as for the previous experiment. The results revealed a significantly lower mortality in larvae treated with PLGA-RIF-NPs than in larvae treated with free RIF.

5 Discussion

As an extension of the pioneering work on NPs done by the Khuller lab, our group has sought to provide a mechanistic explanation for why the PLGA-RIF nanoparticles appear to work better than conventional drugs in treating TB. We propose a model in which the NPs are taken up into the *M.marinum*-infected zebrafish embryos by macrophages that are attracted to the foci of bacterial growth – the granulomas, thereby promoting a natural co-localization between drug and pathogen. This in turn leads to the enhanced therapeutic effect of the drug that is reproducibly seen in our experiments. In order to investigate the validity of this model we have adapted some of the procedures developed by Lalita Ramakrishnans group for the zebrafish embryos. This optically transparent model organism allows us to perform localization experiments wherein we infect the zebrafish embryos with red fluorescent *M.marinum* and later treat it with green fluorescent NPs. Preliminary experiments we performed have quantified the degree of co-localization between NPs and *M.marinum*–positive cells to around 80% [Federico Fenaroli, unpublished results]. Since we chose the zebrafish as our model organism there was a need at the outset to confirm that the reported enhanced therapeutic effect of the NPs seen in mammalian models such as mice and guinea pigs could also be obtained in the zebrafish model. For this, the methodology that I perfected was crucial.

5.1 Main findings

The key finding of this thesis is that NP-treatment decrease the bacterial burden and significantly increase the survivability of zebrafish larvae infected with *M.marinum* relative to free-drug treatment. Importantly, the method I developed allows us now to reproducibly quantify the bacterial load.

The biphasic growth curve of bacterial burden in the larvae treated with free RIF was expected since the literature already emphasizes how free drug is rapidly degraded/excreted from *in-vivo* systems. The biphasic growth curve of our RIF-NPs came as a surprise since the presumed steady release of drug should manifest itself as a stable curtailment of bacterial growth. In a recent release-experiment however it was revealed that about 80% of the RIF-content of the NPs was released within 1 day of exposure to an aqueous environment [Federico Fenaroli, unpublished results]. Currently we have no method to see where the RIF

is located relative to the PLGA-matrix. It could be that a substantial proportion of the drug is located outside rather than inside the NP and that this proportion of drug is rapidly released from the nanoparticle construct. Such an explanation would fit well with the biphasic growth curve seen in experiment 4.4.1 since the RIF beads initially have the same therapeutic effect as free RIF, but after this it has no greater effect than the empty beads. Should this experiment be repeated, one group of embryos should be infected then treated with both free-RIF and empty beads to see if this group would differ from PLGA-RIF beads. However our NPs do not require a sustained release of drug in order to be more effective than free drug. If the NPs are taken up by macrophages before it has released all its contents they would still have an enhanced localized therapeutic effect. Future experiments should try to unveil the kinetics of both NP uptake and RIF-release.

The experiments also reveal that PLGA alone has a pronounced effect on bacterial growth in the infected larvae. Considerable effort has been put into unveiling the immunogenic effects of this polymer [107-109]. It was discovered that the polymer can be used as an adjuvant to increase the effectiveness of vaccines. And indeed, my results indicate that the PLGA enhances the bactericidal activity of immune cells in the zebrafish larvae infected with *M.marinum*.

5.2 E- vs. the M-strain

The E- vs. the M-strain-experiments showed no difference in either mortality or bacterial burden between larvae infected with the two strains. This was unexpected since a striking difference in virulence between the two strains in the adult zebrafish is well-documented [96, 97]. A likely explanation for these findings is that the reported attenuation of the E-strain becomes apparent only in the face of a competent adaptive immune system. Adaptive immunity is present in the adult zebrafish, on which previous experiments have been performed, but absent in the larvae. Had this experiment indicated the same decrease in virulence of the E-strain that has been observed in adult zebrafish, my master thesis could have taken a different direction with identification of genes involved in the pathogenicity of mycobacteria being a main goal of my studies. Since the use of the E-strain would not increase the time-frame in which we could perform measurements on the larvae, we abandoned the idea of using the E-strain as our standard strain for zebrafish infection.

5.3 Fluorescence pixel count is an improvement to the CFU procedure

The development of a robust and sensitive protocol for measuring bacterial burden in zebrafish infected with *M.marinum* was imperative to this research project. The method is an obvious exploitation of our transparent model organism and one that several of our collaborators in the zebrafish community have taken advantage of. The FPC is less labor intensive, higher throughput and more sensitive to low bacterial burden than the CFU protocol. As a result, the FPC has been adopted by several members of our group and can now be considered our standard method for measuring bacterial burden. The CFU procedure remains applicable as a qualitative test for the effectiveness of different infection/treatment-regiments. Our FPC-protocol differs slightly, and is in our opinion an improvement from the one employed by the two most prominent zebrafish-*M.marinum* groups, Meijer and Ramakrishnan, in that it does not only take into account the number of pixels that have fluorescence, but also the intensities of individual pixels. The FPC method has unveiled that there is a huge variability among zebrafish larvae in their ability to cope with mycobacterial infection. As a result we have had to increase the size of sample groups when performing FPC-experiments in order to obtain statistically significant results. Although the procedure is a great improvement to the CFU-protocol, some issues need to be addressed. When presenting results as increase in bacterial burden from initial burden it is important that all negative controls, non-infected fish, have a bacterial burden of zero at all time-points. Out of 74 images of larvae in this particular group, one larva had a FPC-value different from zero. This represents an indefinite increase from the zero-value it held at the previous time-point, and so it had to be omitted from the data-set. Furthermore, in 4 out of $\sim$350 images taken in the whole experiment, the rolling ball subtraction algorithm removed obvious "true" fluorescence signal. Since this problem only affected larvae with an enormous bacterial load with a ratio of true signal/background signal of several orders of magnitude, a rolling ball algorithm was not performed on these larvae.

5.4 The limitations of our model

In the introduction I have tried to make a case for the relevancy of our model to human TB. Nevertheless, our model has certain limitations and these will be addressed in the following section.

In a widely cited paper from 2002 [110], Ramakrishnan proposes a model of *M.marinum*-zebrafish infection wherein infected macrophages extravasate from the blood and into the tissue to form granulomas. Such a model would resemble more the human pulmonary TB than miliary TB. The implication of such a process would be that circulating drugs would have less access to the expanding bacterial population than they would have if the pathogen remained closely associated with the vasculature. In our experiments we have found that the *M.marinum* most often remains near the vasculature (see FIG 8f) where they are easily accessible to circulating drugs like RIF. The efficiency with which the free RIF is able to suppress bacterial growth may thus be overestimated in our experiments compared to its ability suppress bacterial growth in human pulmonary TB. The natural infection route of *M.marinum* into the zebrafish is certainly not through a borosilicate glass needle and it is indeed possible that our intravenous infection protocol affects the localization of bacterial growth as the disease progresses, i.e. it leads to an abnormal infection scenario. Our group is currently trying to establish alternative infection protocols that will more closely recapitulate a natural infection such as intra-peritoneal injection, mimicking the possible uptake of *M.marinum* from the gut, or bath infection, mimicking the possible uptake of *M.marinum* through the skin or the gills. For now, the possibility exists that our model more closely resembles the miliary form of human TB.

In the methods section I describe how we solubilize the free RIF in 5% DMSO prior to injection into the embryo (3.4). This was necessary since RIF is only slightly soluble in water. In addition to being a solvent that dissolves both polar and nonpolar compounds the DMSO is well known for its ability to permeabilize organic tissue [111]. For instance, in medicine it is used as a topical analgesic to facilitate the absorption of drugs into tissues. This effect can also be seen in the zebrafish embryos [112] and is very likely boosting the effect of free RIF. Since DMSO dissolves the PLGA NPs it is not possible to use this solvent for both treatment protocols. The fact that we use a solvent that likely enhances the effect of free drug makes us even more confident that our NPs have additional therapeutic effect.

It is also important to add that the drug treatment in these experiments was administered just once to zebrafish embryos devoid of adaptive immunity and only one day post-infection. In order to cure a human TB patient, even with therapeutic NPs, several doses of treatment would be required and this treatment would in most circumstances be administered after the onset of the adaptive immune response.

5.5 Future of nanoparticle-based therapy

Nanoparticle-based therapy is still in its infancy, but research, including the findings discussed herein, suggests that nano-medicine can help us overcome many of the problems that traditional medicine is facing today. Should we try to anticipate what the future brings in further development in NP-based treatment, we need to consider three factors.

The first factor is the type of polymer used for encapsulation. Since PLGA is not water-soluble there has been great interest in finding alternatives to this polymer in order to avoid the use of any solvents during the manufacturing process. Both chitosan and alginate are being explored, the latter has already been used by the much-cited Khuller to enclose anti-tubercular drugs [113].

The second factor is the type of molecule to be encapsulated and there are many possibilities here. Our group is working towards encapsulating a wide array of agents aimed at TB-treatment. For instance, encapsulation of DNA encoding bactericidal agents such as anti-microbial peptides or encapsulation of efflux pump inhibitors that might have synergistic effects with current drugs [106]. Because of NPs natural ability to target the foci of mycobacterial growth, its application could reduce system toxicity effects compared to free-drug delivery systems. This could in turn make antibiotics that are currently deemed toxic become more attractive for TB therapy. Indeed such compounds have been explored, like capreomycin, a second-line anti-TB drug that is used when the frontline drugs fail [114]. Work is also in progress with encapsulation of *M.tuberculosis* antigens in order to improve on the current BCG-vaccine.

The potential advantages of nanobead-based therapy are not limited to granulomatous diseases like TB. Lasse Evensen in our group is working towards establishing a model wherein he uses NPs to treat cancer in the zebrafish. The zebrafish cancer model is already well-established in some labs [115, 116]. It is commonly known that endothelial cells at the interface between tumor and vasculature are “leaky” [117] thus providing an exit route for intravenously injected molecules such as NPs [118]. This phenomenon is in cancer therapy often referred to as the enhanced permeation and retention effect (EPR). This system could, like our TB-model, display a “natural” co-localization between the drug and its target. In cancer therapy however, we do *not* want NP uptake by phagocytic cells. Modifying the NP-surface by adding polyethylene glycol (PEG) reduces their uptake and clearance by cells of

the mononuclear phagocytic system, leading to prolonged residence time and increased chance that the NPs localize to the tumor [119]. This brings us to the critical third factor; targeting molecules added to the NPs. Since the emergence of antibody-technology, a variety of affinity ligands have been conjugated to NPs in order to increase their specificity. Antibodies, antibody-fragments, peptides, sugars and small peptides have been successfully explored as NP targeting agents [120, 121]. It seems to be a particular advantage of the nanoparticles used against TB that they work well in the absence of special targeting molecules, a consequence of the fact that the macrophages - the site of *M.tuberculosis* residence, are efficient at taking up many different kinds of particles, via 'non-specific' receptors such as the scavenger receptors [10]. Nevertheless, as pointed out by Kalluru et al [56], the NPs in macrophages do not enter the *M.tuberculosis*-phagosome and the NPs may be more efficient when there are targeting molecules such as mannose which, via the mannose receptor may help to target the NPs directly into the *M.tuberculosis*-phagosome.

We are convinced that therapeutic NPs will play a future role in alleviating the burden of TB. Many actual and potential advantages of NP-treatment were nicely summed up in a review from Kamaly et.al 2012, [122], most of which are already described in this thesis: "(1) the ability to improve the pharmaceutical and pharmacological properties of drugs, potentially without the need to alter drug molecules, (2) enhancement of therapeutic efficacy by targeted delivery of drugs in a tissue- or cell-specific manner, (3) delivery of drugs across a range of biological barriers including epithelial and endothelial, (4) delivery of drugs to intracellular sites of action, (5) the ability to deliver multiple types of therapeutics with potentially different physicochemical properties, (6) the ability to deliver a combination of imaging and therapeutic agents for real-time monitoring of therapeutic efficacy and, (7) possibilities to develop highly differentiated therapeutics protected by a unique set of intellectual properties."

5.6 Concluding remarks

The world looks on track to reach WHOs millennium goal of reducing TB incident rates and the Stop TB partnership goal of halving 1990 mortality rates by 2015 [6]. Furthermore, the emergence of several new or re-purposed drugs represents progress that is unparalleled in the last 40 years. But if the success-stories of the 50's and 60's teach us anything, it is that initial progress needs to be followed up by a continual renewal of commitment in order to maintain control of the disease. The emergence of drug-resistant strains of *M.tuberculosis* remains to

be effectively dealt with, but new therapeutic breakthroughs, in particular the use of NPs, could lead the way forward.

Despite the positive world-wide trend of decreasing incident rates, several developing countries have problems with controlling TB. Combined with increasing immigration to the western world, this has resulted in an increase in the number of TB-cases in a developed nation like the UK. In 2011, a total of 8963 new cases of TB were reported, 74% of which were from patients that were born abroad [123]. The trend that the majority of new TB-cases originates from patients that have been born, and likely contracted the disease abroad is seen in many western countries [6], and it serves to underscore what will be the final point made in this thesis; that failure to control TB anywhere translates into failure to truly control TB everywhere.

6 Appendix

6.1 Statistics

P<0.05 deemed differences significant in all statistical tests.

All survival experiments were analyzed for significant differences with a Log Rank (Mantel-Cox) test with Graphpad Prism® version 5

In the bacterial burden FPC experiment (4.4.1) we looked for differences in bacterial growth using the Linear Mixed Effect model (LME) with the statistics software "R". To analyze differences between groups at single time-points we used a one-way Anova with students Newman-Keuls post hoc test in Graphpad Prism ® version 5.

6.2 Calculations

Calculating the volume and concentration of RIF, PLGA-RIF NPs and PLGA NPs to be injected into the zebrafish embryos

RIF

1x human dose of RIF = 12mgRIF/kgTissue

The zebrafish weighs about 1.2mg so in order to have the same drug/tissue-weight ratio as the 1x human dose we require 12mgRIF/kgTissue x $1.2x10^{-6}$kgTissue = $14.4x10^{-6}$ mg RIF

We use 1mg RIF in 213µL 5%DMSO solution to get a **4.7mg/mL RIF solution**. We need to inject $14.4x10^{-6}$mg / 4.7mg/mL **= 3.1nL RIF suspension**

PLGA-RIF NPs

Since our NPs had a drug loading of 34% (RIF/(RIF+PLGA)) we ~tripled the concentration in order to get the same amount of RIF into the embryo. Instead of using 1mg in 213µL suspension as we did with the RIF, we used 1mg PLGA-RIF in 71µL suspension to get a **14.1mg/mL PLGA-RIF NP solution** then injected the same amount **= 3.1nL PLGA-RIF suspension**

PLGA NPs

Our PLGA-RIF NPs had a drug loading of 34%, meaning 66% of the weight was from PLGA. We needed to inject a solution of concentration 0.66 x 14.1 mg/mL **=9.3mg/mL PLGA suspension** which was easily done by using 1mg PLGA in (1000/9.3) 108 µL solution. We then injected the same amount **= 3.1nL PLGA- solution.**

Calculating ΔLog_{10} FPC values

The FPC values were Log_{10}-transformed, and for each larva, the difference between each day's measurement and the initial bacterial burden was calculated. The growth of bacterial burden over defined intervals was calculated by taking the mean and SEM of the ΔLog_{10} FPC values calculated for individual larvae. All FPC-values of 0 were set to 1 to allow Log_{10}-transformation.

6.3 Bacterial strains

The M-strain DS-Red *Mycobacterium marinum* was a personal gift from Nathalie Winter and Brigitte Gicquel of Institut Pasteur, Paris – France.

The E-strain DS-Red *Mycobacterium marinum* (strain E-11) was a personal gift from Annemarie Meijer of the University of Leiden, Leiden – The Netherlands.

6.4 Recipes

Deionized, distilled water was used in all recipes and protocol steps

7H9 liquid culture medium

Adapted from Cosma et.al 2006 [98]

4.7 g Middlebrook 7H9 broth base (Difco)

4 ml 50% (v/v) glycerol

Dissolve the broth base in water, add glycerol, bring to final volume of 900 ml, autoclave. Store up to 3 months at room temperature. Before use, add 100 ml ADC stock (see recipe) and 2.5 ml of 20% (v/v) Tween 80. Store up to 2 months at 4◦C

7H10 agar plates

Adapted from Cosma et.al 2006 [98]

19 g Middlebrook 7H10 base (Difco)

10 ml 50% (v/v) glycerol

Dissolve the broth base in water, add glycerol, and bring to final volume of 900 ml. Autoclave, allow cooling to ∼42◦C. Add 100 ml ADC supplement (see recipe). Pour ∼35, 100 × 15−mm plates. Store up to 2 months at 4◦C

Supplements to 7H10 agar plates

Adapted from Cosma et.al 2006 [98]

40 ml 250 µg/ml amphotericin B stock (Sigma-Aldrich)

500 µl 50 mg/ml polymixin B sulphate (Sigma-Aldrich)

400 µl 50 mg/ml trimethoprim (Sigma-Aldrich)

1 ml 50 mg/ml carbenecillin, disodium salt (Sigma-Aldrich)

Store amphotericin B, polymixin B, trimethoprim and carbenecillin stocks up to 1 year at −20◦C

Supplements are formulated per liter of 7H10 agar plates.

Hanks' stock solutions

Adapted from Westerfield 2000 [75].

Stock #1:

8.0 g NaCl

0.4 g KCl

100 ml H2O

Stock #2:

0.358 g Na2HPO4 anhydrous

0.60 g KH2PO4

100 ml H2O

Stock #4:

0.72 g CaCl2

50 ml H2O

Stock #5:

1.23 g MgSO4·7H2O

50 ml H2O

Stock #6:

0.35 g NaHCO3

10 ml H2O

All of Hanks' stock solutions should be stored indefinitely at 4◦C.

ADC supplement

Adapted from Cosma et.al 2006 [98]

Dissolve the following in ~700 ml H2O:

50 g BSA, fraction V (Sigma-Aldrich)

20 g dextrose

8.5 g NaCl

Bring to 1 liter final volume. Filter-sterilize using a 0.22-µm filter. Store up to 6 months at 4◦C

Tricaine stock solution

Adapted from Cosma et.al 2006 [98].

400 mg tricaine (Argent Laboratories)

97.9 ml H2O

~2.1 ml 1 M Tris·Cl, pH 9

Adjust pH to ~7

Store up to 1 month at 4◦C

Adapted

Zebrafish embryo medium

Adapted from Westerfield 2000 [75].

1.0 ml Hanks' stock solution #1 (see recipe)

0.1 ml Hanks' stock solution #2 (see recipe)

1.0 ml Hanks' stock solution #4 (see recipe)

95.9 ml H_2O

1.0 ml Hanks' stock solution #5 (see recipe)

1.0 ml Hanks' stock solution #6 (see recipe)

Use about ten drops 1 M NaOH to pH 7.2. Store indefinitely at 4◦C

7 References

1. Soled, M., *Aphorisms of Hippocrates.* N J Med, 1991. **88**(1): p. 33.
2. Zink, A.R., et al., *Characterization of Mycobacterium tuberculosis complex DNAs from Egyptian mummies by spoligotyping.* J Clin Microbiol, 2003. **41**(1): p. 359-67.
3. Daniel, T.M., *The history of tuberculosis.* Respir Med, 2006. **100**(11): p. 1862-70.
4. Koch, R., M. Pinner, and B.R. Pinner, *The aetiology of tuberculosis*. 1932, New York city,: National tuberculosis association.
5. Calmette, A., *On preventive vaccination of the new-born against tuberculosis by B.C.G.* British Journal of Tuberculosis, 1928. **22**(4): p. 161-165.
6. *Global Tuberculosis Report 2012*. Global Tuberculosis report. 2012, Geneva: World Health Organization.
7. Enarson, D.A. and N. Ait-Khaled, *[Principles and organization of tuberculosis control]*. Rev Prat, 1996. **46**(11): p. 1368-73.
8. *Tuberculosis fact sheet: General information*, 2012, CDC - Centers for Disease Control and Prevention: http://www.cdc.gov/tb/publications/factsheets/general/tb.htm.
9. Dannenberg, A.M., Jr., *Immunopathogenesis of pulmonary tuberculosis.* Hosp Pract (Off Ed), 1993. **28**(1): p. 51-8.
10. Ernst, J.D., *Macrophage receptors for Mycobacterium tuberculosis.* Infect Immun, 1998. **66**(4): p. 1277-81.
11. Pugin, J., et al., *CD14 Is a pattern recognition receptor.* Immunity, 1994. **1**(6): p. 509-516.
12. Downing, J.F., et al., *Surfactant protein a promotes attachment of Mycobacterium tuberculosis to alveolar macrophages during infection with human immunodeficiency virus.* Proceedings of the National Academy of Sciences, 1995. **92**(11): p. 4848-4852.
13. Schlesinger, L.S., et al., *Phagocytosis of Mycobacterium tuberculosis is mediated by human monocyte complement receptors and complement component C3.* The Journal of Immunology, 1990. **144**(7): p. 2771-80.
14. Schlesinger, L.S., *Macrophage phagocytosis of virulent but not attenuated strains of Mycobacterium tuberculosis is mediated by mannose receptors in addition to complement receptors.* The Journal of Immunology, 1993. **150**(7): p. 2920-30.
15. Means, T.K., et al., *Human Toll-Like Receptors Mediate Cellular Activation by Mycobacterium tuberculosis.* The Journal of Immunology, 1999. **163**(7): p. 3920-3927.
16. Dunne, D.W., et al., *The type I macrophage scavenger receptor binds to gram-positive bacteria and recognizes lipoteichoic acid.* Proceedings of the National Academy of Sciences, 1994. **91**(5): p. 1863-1867.
17. Ulrichs, T. and S.H.E. Kaufmann, *New insights into the function of granulomas in human tuberculosis.* Journal of Pathology, 2006. **208**(2): p. 261-269.
18. Davis, J.M. and L. Ramakrishnan, *The Role of the Granuloma in Expansion and Dissemination of Early Tuberculous Infection.* Cell, 2009. **136**(1): p. 37-49.
19. Adams, D.O., *The granulomatous inflammatory response. A review.* Am J Pathol, 1976. **84**(1): p. 164-92.
20. Wolf, A.J., et al., *Mycobacterium tuberculosis Infects Dendritic Cells with High Frequency and Impairs Their Function In Vivo.* The Journal of Immunology, 2007. **179**(4): p. 2509-2519.

21. Cooper, A.M., *Cell-mediated immune responses in tuberculosis.* Annu Rev Immunol, 2009. **27**: p. 393-422.
22. Harries, A.D. *TB/HIV a clinical manual*. 2004; Available from: http://public.eblib.com/EBLPublic/PublicView.do?ptiID=284591.
23. Hussain, S.F., et al., *Clinical characteristics of 110 miliary tuberculosis patients from a low HIV prevalence country.* Int J Tuberc Lung Dis, 2004. **8**(4): p. 493-9.
24. Lawn, S.D. and A.I. Zumla, *Tuberculosis.* The Lancet. **378**(9785): p. 57-72.
25. Russell, D.G., et al., *Foamy macrophages and the progression of the human tuberculosis granuloma.* Nat Immunol, 2009. **10**(9): p. 943-8.
26. Parrish, N.M., J.D. Dick, and W.R. Bishai, *Mechanisms of latency in Mycobacterium tuberculosis.* Trends in Microbiology, 1998. **6**(3): p. 107-112.
27. Harbitz, F., *Om oprindelsen til og utviklingen av de tuberkuløse sygdommer: (tuberkulosens ætiologi og patogenese) : med bemerkninger om profylaxen : en oversikt for læger og studerende*. 1922, Kristiania: Den norske nationalforeningen mot tuberkulosen. 96 s., pl. : ill.
28. Russell, D.G., C.E. Barry, 3rd, and J.L. Flynn, *Tuberculosis: what we don't know can, and does, hurt us.* Science, 2010. **328**(5980): p. 852-6.
29. Gedde-Dahl, T., *Tuberculous infection in the light of tuberculin matriculation.* Am J Hyg, 1952. **56**(2): p. 139-214.
30. Flynn, J.L., *Lessons from experimental Mycobacterium tuberculosis infections.* Microbes Infect, 2006. **8**(4): p. 1179-88.
31. Russell, D.G., *Who puts the tubercle in tuberculosis?* Nat Rev Microbiol, 2007. **5**(1): p. 39-47.
32. Egen, J.G., et al., *Macrophage and T Cell Dynamics during the Development and Disintegration of Mycobacterial Granulomas.* Immunity, 2008. **28**(2): p. 271-284.
33. Cosma, C.L., O. Humbert, and L. Ramakrishnan, *Superinfecting mycobacteria home to established tuberculous granulomas.* Nat Immunol, 2004. **5**(8): p. 828-835.
34. Cosma, C.L., et al., *Trafficking of Superinfecting Mycobacterium Organisms into Established Granulomas Occurs in Mammals and Is Independent of the Erp and ESX-1 Mycobacterial Virulence Loci.* Journal of Infectious Diseases, 2008. **198**(12): p. 1851-1855.
35. Via, L.E., et al., *Tuberculous Granulomas Are Hypoxic in Guinea Pigs, Rabbits, and Nonhuman Primates.* Infection and Immunity, 2008. **76**(6): p. 2333-2340.
36. Orme, I.M., *The immunopathogenesis of tuberculosis: a new working hypothesis.* Trends in Microbiology, 1998. **6**(3): p. 94-97.
37. Barker, L.P., et al., *Differential trafficking of live and dead Mycobacterium marinum organisms in macrophages.* Infect Immun, 1997. **65**(4): p. 1497-504.
38. Sturgill-Koszycki, S., et al., *Lack of acidification in Mycobacterium phagosomes produced by exclusion of the vesicular proton-ATPase.* Science, 1994. **263**(5147): p. 678-681.
39. Ullrich, H.-J., W.L. Beatty, and D.G. Russell, *Direct delivery of procathepsin D to phagosomes: Implications for phagosome biogenesis and parasitism by Mycobacterium.* European Journal of Cell Biology, 1999. **78**(10): p. 739-748.
40. Malik, Z.A., G.M. Denning, and D.J. Kusner, *Inhibition of Ca(2+) signaling by Mycobacterium tuberculosis is associated with reduced phagosome-lysosome fusion and increased survival within human macrophages.* J Exp Med, 2000. **191**(2): p. 287-302.
41. Fratti, R.A., et al., *Role of phosphatidylinositol 3-kinase and Rab5 effectors in phagosomal biogenesis and mycobacterial phagosome maturation arrest.* J Cell Biol, 2001. **154**(3): p. 631-44.

42. Ferrari, G., et al., *A Coat Protein on Phagosomes Involved in the Intracellular Survival of Mycobacteria.* Cell, 1999. **97**(4): p. 435-447.
43. Anes, E., et al., *Selected lipids activate phagosome actin assembly and maturation resulting in killing of pathogenic mycobacteria.* Nat Cell Biol, 2003. **5**(9): p. 793-802.
44. Via, L.E., et al., *Arrest of mycobacterial phagosome maturation is caused by a block in vesicle fusion between stages controlled by rab5 and rab7.* Journal of Biological Chemistry, 1997. **272**(20): p. 13326-13331.
45. Flynn, J.L. and J. Chan, *Immune evasion by Mycobacterium tuberculosis: living with the enemy.* Curr Opin Immunol, 2003. **15**(4): p. 450-5.
46. Schaible, U.E., et al., *Cytokine activation leads to acidification and increases maturation of Mycobacterium avium-containing phagosomes in murine macrophages.* J Immunol, 1998. **160**(3): p. 1290-6.
47. Armstrong, J.A. and P.D. Hart, *Phagosome-lysosome interactions in cultured macrophages infected with virulent tubercle bacilli. Reversal of the usual nonfusion pattern and observations on bacterial survival.* J Exp Med, 1975. **142**(1): p. 1-16.
48. Salyers, A.A. and D.D. Whitt, *Microbiology: diversity, disease, and the environment*. 2001: Fitzgerald Science Press.
49. Escribano, I., et al., *Importance of the Efflux Pump Systems in the Resistance of Mycobacterium tuberculosis to Fluoroquinolones and Linezolid.* Chemotherapy, 2007. **53**(6): p. 397-401.
50. Romeyn, J.A., *Exogenous reinfection in tuberculosis.* Am Rev Respir Dis, 1970. **101**(6): p. 923-7.
51. Black, G.F., et al., *BCG-induced increase in interferon-gamma response to mycobacterial antigens and efficacy of BCG vaccination in Malawi and the UK: two randomised controlled studies.* Lancet, 2002. **359**(9315): p. 1393-401.
52. Verma, I. and A. Grover, *Antituberculous vaccine development: a perspective for the endemic world.* Expert Rev Vaccines, 2009. **8**(11): p. 1547-53.
53. Behr, M.A.S., Peter M., *Has BCG attenuated to impotence?* Nature, 1997. **389**(6647).
54. Brandt, L., et al., *Failure of the Mycobacterium bovis BCG vaccine: some species of environmental mycobacteria block multiplication of BCG and induction of protective immunity to tuberculosis.* Infect Immun, 2002. **70**(2): p. 672-8.
55. Sharma, A., et al., *Chemotherapeutic efficacy of poly (DL-lactide-co-glycolide) nanoparticle encapsulated antitubercular drugs at sub-therapeutic dose against experimental tuberculosis.* Int J Antimicrob Agents, 2004. **24**(6): p. 599-604.
56. Kalluru, R., et al., *Polylactide-co-glycolide-rifampicin-nanoparticles efficiently clear Mycobacterium bovis BCG infection in macrophages and remain membrane-bound in phago-lysosomes.* J Cell Sci, 2013.
57. Desjardins, M. and G. Griffiths, *Phagocytosis: latex leads the way.* Curr Opin Cell Biol, 2003. **15**(4): p. 498-503.
58. Dutt, M. and G.K. Khuller, *Chemotherapy of Mycobacterium tuberculosis infections in mice with a combination of isoniazid and rifampicin entrapped in Poly (DL-lactide-co-glycolide) microparticles.* Journal of Antimicrobial Chemotherapy, 2001. **47**(6): p. 829-835.
59. Dutt, M. and G.K. Khuller, *Therapeutic efficacy of poly(DL-lactide-co-glycolide)-encapsulated antitubercular drugs against Mycobacterium tuberculosis infection induced in mice.* Antimicrobial Agents and Chemotherapy, 2001. **45**(1): p. 363-366.
60. Pandey, R., et al., *Poly (DL-lactide-co-glycolide) nanoparticle-based inhalable sustained drug delivery system for experimental tuberculosis.* Journal of Antimicrobial Chemotherapy, 2003. **52**(6): p. 981-986.

61. Pandey, R., et al., *Nanoparticle encapsulated antitubercular drugs as a potential oral drug delivery system against murine tuberculosis.* Tuberculosis, 2003. **83**(6): p. 373-378.
62. Calvori, C., et al., *Effect of rifamycin on protein synthesis.* Nature, 1965. **207**(995): p. 417-8.
63. Shive, M.S. and J.M. Anderson, *Biodegradation and biocompatibility of PLA and PLGA microspheres.* Adv Drug Deliv Rev, 1997. **28**(1): p. 5-24.
64. Bowman, K. and K.W. Leong, *Chitosan nanoparticles for oral drug and gene delivery.* Int J Nanomedicine, 2006. **1**(2): p. 117-28.
65. Ahmad, Z. and G.K. Khuller, *Alginate-based sustained release drug delivery systems for tuberculosis.* Expert Opinion on Drug Delivery, 2008. **5**(12): p. 1323-1334.
66. Koul, A., et al., *Interplay between mycobacteria and host signalling pathways.* Nature Reviews Microbiology, 2004. **2**(3): p. 189-202.
67. Dionne, M.S., N. Ghori, and D.S. Schneider, *Drosophila melanogaster is a genetically tractable model host for Mycobacterium marinum.* Infection and Immunity, 2003. **71**(6): p. 3540-3550.
68. Hagedorn, M. and T. Soldati, *Flotillin and RacH modulate the intracellular immunity of Dictyostelium to Mycobacterium marinum infection.* Cell Microbiol, 2007. **9**(11): p. 2716-33.
69. Capuano, S.V., et al., *Experimental Mycobacterium tuberculosis Infection of Cynomolgus Macaques Closely Resembles the Various Manifestations of Human M. tuberculosis Infection.* Infection and Immunity, 2003. **71**(10): p. 5831-5844.
70. O'Toole, R., *Experimental Models Used to Study Human Tuberculosis.* Advances in Applied Microbiology, Vol 71, 2010. **71**: p. 75-89.
71. Padilla-Carlin, D.J., D.N. McMurray, and A.J. Hickey, *The Guinea Pig as a Model of Infectious Diseases.* Comparative Medicine, 2008. **58**(4): p. 324-340.
72. Manabe, Y.C., et al., *Different strains of Mycobacterium tuberculosis cause various spectrums of disease in the rabbit model of tuberculosis.* Infect Immun, 2003. **71**(10): p. 6004-11.
73. Swaim, L.E., et al., *Mycobacterium marinum infection of adult zebrafish causes caseating granulomatous tuberculosis and is moderated by adaptive immunity (vol 74, pg 6108, 2006).* Infection and Immunity, 2007. **75**(3): p. 1540-1540.
74. Laale, H.W., *Biology and Use of Zebrafish, Brachydanio-Rerio in Fisheries Research - Literature-Review.* Journal of Fish Biology, 1977. **10**(2): p. 121-&.
75. Westerfield, M., *The zebrafish book. A guide for the laboratory use of zebrafish (Danio rerio). 4th ed. University of Oregon Press, Eugene.* 2000.
76. Alestrom, P., J.L. Holter, and R. Nourizadeh-Lillabadi, *Zebrafish in functional genomics and aquatic biomedicine.* Trends Biotechnol, 2006. **24**(1): p. 15-21.
77. Kimmel, C.B., *Genetics and early development of zebrafish.* Trends Genet, 1989. **5**(8): p. 283-8.
78. Howe, K., et al., *The zebrafish reference genome sequence and its relationship to the human genome.* Nature, 2013.
79. Traver, D., et al., *The Zebrafish as a Model Organism to Study Development of the Immune System*, in *Advances in Immunology*. 2003, Academic Press. p. 254-330.
80. Jault, C., L. Pichon, and J. Chluba, *Toll-like receptor gene family and TIR-domain adapters in Danio rerio.* Mol Immunol, 2004. **40**(11): p. 759-71.
81. Gongora, R., F. Figueroa, and J. Klein, *Independent duplications of Bf and C3 complement genes in the zebrafish.* Scand J Immunol, 1998. **48**(6): p. 651-8.

82. Swaim, L.E., et al., *Mycobacterium marinum infection of adult zebrafish causes caseating granulomatous tuberculosis and is moderated by adaptive immunity.* Infect Immun, 2006. **74**(11): p. 6108-17.
83. Saunders, B.M., H. Briscoe, and W.J. Britton, *T cell-derived tumour necrosis factor is essential, but not sufficient, for protection against Mycobacterium tuberculosis infection.* Clin Exp Immunol, 2004. **137**(2): p. 279-87.
84. Langenau, D.M., et al., *In vivo tracking of T cell development, ablation, and engraftment in transgenic zebrafish.* Proc Natl Acad Sci U S A, 2004. **101**(19): p. 7369-74.
85. Ramakrishnan, L., et al., *Mycobacterium marinum causes both long-term subclinical infection and acute disease in the leopard frog (Rana pipiens).* Infection and Immunity, 1997. **65**(2): p. 767-773.
86. Cirillo, J.D., et al., *Interaction of Mycobacterium avium with environmental amoebae enhances virulence.* Infect Immun, 1997. **65**(9): p. 3759-67.
87. Linell, F. and A. Norden, *Mycobacterium balnei, a new acid-fast bacillus occurring in swimming pools and capable of producing skin lesions in humans.* Acta Tuberc Scand Suppl, 1954. **33**: p. 1-84.
88. Norden, A. and F. Linell, *A new type of pathogenic Mycobacterium.* Nature, 1951. **168**(4280): p. 826.
89. Tonjum, T., et al., *Differentiation of Mycobacterium ulcerans, M. marinum, and M. haemophilum: mapping of their relationships to M. tuberculosis by fatty acid profile analysis, DNA-DNA hybridization, and 16S rRNA gene sequence analysis.* J Clin Microbiol, 1998. **36**(4): p. 918-25.
90. Clay, H., et al., *Dichotomous role of the macrophage in early Mycobacterium marinum infection of the zebrafish.* Cell Host & Microbe, 2007. **2**(1): p. 29-39.
91. Clay, H., H.E. Volkman, and L. Ramakrishnan, *Tumor Necrosis Factor Signaling Mediates Resistance to Mycobacteria by Inhibiting Bacterial Growth and Macrophage Death.* Immunity, 2008. **29**(2): p. 283-294.
92. Stinear, T.P., et al., *Insights from the complete genome sequence of Mycobacterium marinum on the evolution of Mycobacterium tuberculosis.* Genome Res, 2008. **18**(5): p. 729-41.
93. Ruley, K.M., et al., *Identification of Mycobacterium marinum virulence genes using signature-tagged mutagenesis and the goldfish model of mycobacterial pathogenesis.* Fems Microbiology Letters, 2004. **232**(1): p. 75-81.
94. Mehta, P.K., et al., *Identification of Mycobacterium marinum macrophage infection mutants.* Microbial Pathogenesis, 2006. **40**(4): p. 139-151.
95. Collins, F.M., V. Montalbine, and N.E. Morrison, *Growth and immunogenicity of photochromogenic strains of mycobacteria in the footpads of normal mice.* Infect Immun, 1975. **11**(5): p. 1079-87.
96. van der Sar, A.M., et al., *Mycobacterium marinum Strains Can Be Divided into Two Distinct Types Based on Genetic Diversity and Virulence.* Infection and Immunity, 2004. **72**(11): p. 6306-6312.
97. Meijer, A.H., et al., *Transcriptome profiling of adult zebrafish at the late stage of chronic tuberculosis due to Mycobacterium marinum infection.* Mol Immunol, 2005. **42**(10): p. 1185-203.
98. Cosma, C.L., et al., *Zebrafish and frog models of Mycobacterium marinum infection.* Curr Protoc Microbiol, 2006. **Chapter 10**: p. Unit 10B 2.
99. Benard, E.L., et al., *Infection of zebrafish embryos with intracellular bacterial pathogens.* J Vis Exp, 2012(61).

100. Schindelin, J., et al., *Fiji: an open-source platform for biological-image analysis.* Nat Methods, 2012. **9**(7): p. 676-82.
101. Castle, M. and J. Keller, *Rolling Ball Background Java*, 2007. p. http://rsb.info.nih.gov/ij/plugins/rolling-ball.html.
102. Bolte, S. and F.P. Cordelieres, *A guided tour into subcellular colocalization analysis in light microscopy.* Journal of Microscopy-Oxford, 2006. **224**: p. 213-232.
103. Mitchison, D.A., et al., *A selective oleic acid albumin agar medium for tubercle bacilli.* J Med Microbiol, 1972. **5**(2): p. 165-75.
104. Somoskovi, A. and P. Magyar, *Comparison of the mycobacteria growth indicator tube with MB redox, Lowenstein-Jensen, and Middlebrook 7H11 media for recovery of mycobacteria in clinical specimens.* J Clin Microbiol, 1999. **37**(5): p. 1366-9.
105. Lindeboom, J.A., et al., *Clinical manifestations, diagnosis, and treatment of Mycobacterium haemophilum infections.* Clin Microbiol Rev, 2011. **24**(4): p. 701-17.
106. Adams, K.N., et al., *Drug tolerance in replicating mycobacteria mediated by a macrophage-induced efflux mechanism.* Cell, 2011. **145**(1): p. 39-53.
107. Jiang, W., et al., *Biodegradable poly(lactic-co-glycolic acid) microparticles for injectable delivery of vaccine antigens.* Advanced Drug Delivery Reviews, 2005. **57**(3): p. 391-410.
108. Nicolete, R., D.F.d. Santos, and L.H. Faccioli, *The uptake of PLGA micro or nanoparticles by macrophages provokes distinct in vitro inflammatory response.* International Immunopharmacology, 2011. **11**(10): p. 1557-1563.
109. O'Hagan, D.T. and M. Singh, *Microparticles as vaccine adjuvants and delivery systems.* Expert Review of Vaccines, 2003. **2**(2): p. 269-283.
110. Davis, J.M., et al., *Real-Time Visualization of Mycobacterium-Macrophage Interactions Leading to Initiation of Granuloma Formation in Zebrafish Embryos.* Immunity, 2002. **17**(6): p. 693-702.
111. Puig Muset, P. and J. Martin-Esteve, *Physiological cell permeability and pharmacological action of DMSO.* Experientia, 1965. **21**(11): p. 649-51.
112. Maes, J., et al., *Evaluation of 14 organic solvents and carriers for screening applications in zebrafish embryos and larvae.* PLoS One, 2012. **7**(10): p. e43850.
113. Zahoor, A., S. Sharma, and G.K. Khuller, *Inhalable alginate nanoparticles as antitubercular drug carriers against experimental tuberculosis.* International Journal of Antimicrobial Agents, 2005. **26**(4): p. 298-303.
114. Garcia-Contreras, L., et al., *Inhaled large porous particles of capreomycin for treatment of tuberculosis in a guinea pig model.* Antimicrob Agents Chemother, 2007. **51**(8): p. 2830-6.
115. He, S., et al., *Neutrophil-mediated experimental metastasis is enhanced by VEGFR inhibition in a zebrafish xenograft model.* J Pathol, 2012. **227**(4): p. 431-45.
116. He, S., et al., *A ΔRaf1–ER-inducible oncogenic zebrafish liver cell model identifies hepatocellular carcinoma signatures.* The Journal of Pathology, 2011. **225**(1): p. 19-28.
117. Peterson, H.I. and L. Appelgren, *Tumour vessel permeability and transcapillary exchange of large molecules of different size.* Bibl Anat, 1977(15 Pt 1): p. 262-5.
118. Jain, R.K., *Transport of molecules across tumor vasculature.* Cancer Metastasis Rev, 1987. **6**(4): p. 559-93.
119. Wattendorf, U. and H.P. Merkle, *PEGylation as a tool for the biomedical engineering of surface modified microparticles.* Journal of Pharmaceutical Sciences, 2008. **97**(11): p. 4655-4669.
120. Heath, T.D., et al., *Antibody-targeted liposomes: increase in specific toxicity of methotrexate-gamma-aspartate.* Proc Natl Acad Sci U S A, 1983. **80**(5): p. 1377-81.

121. Leserman, L.D., et al., *Targeting to cells of fluorescent liposomes covalently coupled with monoclonal antibody or protein A.* Nature, 1980. **288**(5791): p. 602-4.
122. Kamaly, N., et al., *Targeted polymeric therapeutic nanoparticles: design, development and clinical translation.* Chem Soc Rev, 2012. **41**(7): p. 2971-3010.
123. *Annual report on tuberculosis surveillance in the UK, 2012*. Tuberculosis in the UK. 2012, London: Health Protection Agency.